



Sooty terns as large-scale bioindicator of mercury contamination in marine ecosystems: A pantropical approach

Fanny Cusset^{a,b,*}, Mickaël Charriot^a, Pierre Richard^a, Jérôme Fort^a, Leandro Bugoni^c, Nicholas Carlile^d, Annabelle Cupidon^e, Nina da Rocha^f, Antonio Garcia-Quintas^{g,h}, Gaël Guillou^a, Matthew Morgan^e, Terence O'Dwyerⁱ, Patricia Luciano Mancini^j, Verónica Costa Neves^k, Gerard Rocamora^l, Laura Shearer^m, Eduardo Ventosaⁿ, Yves Cherel^b, Paco Bustamante^{a,o}

^a Littoral Environnement et Sociétés (LIENSs), UMR 7266 CNRS - La Rochelle Université, 2 rue Olympe de Gouges, La Rochelle 17000, France

^b Centre d'Études Biologiques de Chizé (CEBC), UMR 7372 CNRS - La Rochelle Université, Villiers-en Bois 79360, France

^c Instituto de Ciências Biológicas, Universidade Federal do Rio Grande (FURG), Brazil

^d Æstrelata Restorations, Kangaroo Valley, Australia

^e Island Conservation Society, P.O. Box 775, Victoria, Pointe Larue, Mahé, Seychelles

^f Fundação Píncipe, Santo António, Ilha do Príncipe, Democratic Republic of Sao Tome and Principe

^g Université de Bretagne Occidentale, UMR LEMAR (UBO, CNRS, IRD, Ifremer), Plouzané, France

^h Centro de Investigaciones de Ecosistemas Costeros, Cayo Coco, Cuba

ⁱ Gadfly Ecological Services, Brisbane, Australia

^j Instituto de Biodiversidade e Sustentabilidade NUPEM, Universidade Federal do Rio De Janeiro, Av. Amaro Reinaldo dos Santos Silva, 764, São José do Barreto, Macé 27965-045, Brazil

^k Instituto de Investigação em Ciências do Mar – OKEANOS, University of the Azores, Horta 9900-138, Portugal

^l Island Biodiversity and Conservation centre, University of Seychelles, P.O. Box 1348, Anse Royale, Mahé, Seychelles

^m Ascension Island Government Conservation and Fisheries Directorate (AIGCFD), Ascension Island, South Atlantic Ocean, Georgetown, USA

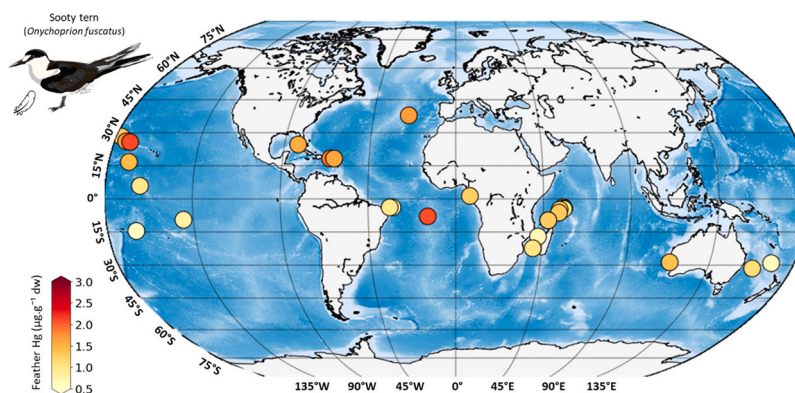
ⁿ Effective Environment Restoration, Monte Rico St Carite D6, Cabo Rojo, PR 00623, Puerto Rico

^o Institut Universitaire de France (IUF), 1 rue Descartes, Paris 75005, France

HIGHLIGHTS

- Sooty terns were used to monitor Hg contamination across tropical oceans worldwide.
- Higher concentrations were found in the Northern Hemisphere and the Atlantic Ocean.
- CSIA-AA-derived trophic position for adults were similar among colonies.
- Drivers included environmental contamination rather than diet.
- Feather Hg levels were higher in the 2020s than previously documented.

GRAPHICAL ABSTRACT



* Corresponding author at: Littoral Environnement et Sociétés (LIENSs), UMR 7266 CNRS - La Rochelle Université, 2 rue Olympe de Gouges, La Rochelle 17000, France.

E-mail addresses: cussetfanny@gmail.com, fanny.cusset@npolar.no (F. Cusset).

<https://doi.org/10.1016/j.jhazmat.2026.141530>

Received 25 October 2025; Received in revised form 13 February 2026; Accepted 16 February 2026

Available online 17 February 2026

0304-3894/© 2026 The Authors. Published by Elsevier B.V. This is an open access article under the CC BY license (<http://creativecommons.org/licenses/by/4.0/>).

ARTICLE INFO

Keywords:

Hg
Spatial biomonitoring
Seabirds
Feathers
Stable isotopes
CSIA-AA
Onychoprion fuscatus

ABSTRACT

Mercury (Hg) is a toxic contaminant, which poses serious threats to both wildlife and humans worldwide. Although tropical oceans receive half of the world's atmospheric Hg depositions, its biomonitoring is largely overlooked in these ecosystems. This study provides a comprehensive, pantropical assessment of Hg contamination of marine ecosystems, using the sooty tern (*Onychoprion fuscatus*) as bioindicator. Total Hg concentrations were measured from feathers collected in 28 colonies across all tropical oceans (2003–2022), from adults (n = 564) and chicks (n = 407), to evaluate longer- and shorter-term contamination. To investigate the role of bird trophic ecology on Hg contamination, bulk stable isotopes of carbon ($\delta^{13}\text{C}$) and nitrogen ($\delta^{15}\text{N}$) were also analysed, as respective proxies for feeding habitat and diet. Because baselines of stable isotopes may vary at large spatial scales, compound-specific nitrogen stable isotope analyses of amino-acids were performed on a subset of adults (n = 91, 19 colonies), to calculate their trophic position (TP), accounting for both baseline and trophic effects. As expected, Hg concentrations were higher in adults than chicks, because of their shorter bioaccumulation period. Overall, colonies from the Northern Hemisphere exhibited the highest Hg concentrations, consistently with higher historical anthropogenic emissions of Hg in the North. Models revealed that Hg contamination was driven by environmental contamination (colony location, feeding habitat) rather than diet (TP), which remained similar across the pantropical range. Our findings provide important baseline data for tropical marine ecosystems and underscore the need for enhanced monitoring in regions, where gold-mining and changing oceanographic conditions will likely modify future Hg exposure.

1. Introduction

From both natural and anthropogenic origin, mercury (Hg) is recognized as a major contaminant of public health concern (WHO, 2020), due to its adverse effects on human and environmental health when above natural concentrations. To address this threat, the United Nations Environment Programme (UNEP) has produced successive Global Mercury Assessments, providing a comprehensive overview of the current knowledge on Hg at the global scale. In its latest 2018 assessment, oceans were identified as «locations of greatest concern». Indeed, oceans are primary reservoirs of Hg, allowing its storage over long periods and its subsequent re-emissions over time [1,2]. After its release and large-scale transport in the atmosphere, Hg deposits in oceans all over the globe [3]. There, Hg is efficiently transformed to its most toxic and bioavailable form, methyl-Hg (MeHg), by naturally-occurring microorganisms [4]. Methyl-Hg accumulates in marine biota (*i.e.*, concentrations increase in tissues over time), thus causing numerous negative health effects (*e.g.*, neurological, developmental, reproductive or immunological) on affected organisms [5–9], as well as soil contamination in islands hosting seabird colonies [10]. Once assimilated by phytoplankton, MeHg is transferred along marine food chains [11], where it readily biomagnifies (*i.e.*, concentrations increase from primary producers to top predators). Due to both marine methylation and the huge surface and volume of seawater, the world's oceans promote the bioavailability and toxicity of MeHg, thus posing serious threats to both wildlife and humans that heavily rely on marine resources [12].

Overall, oceans receive about 80 % of total atmospheric Hg depositions, 49 % of which are restricted to the tropics [13]. Yet, Hg monitoring remains largely overlooked in tropical waters [14], especially in the Southern Hemisphere (SH), and were recently identified as regions where Hg data and scientific understanding are most lacking ([15–17]). Still, the intertropical region includes most countries where artisanal and small-scale gold mining occurs [18]. This growing activity represents the largest user and emitter of Hg globally, producing more than 35 % of total atmospheric Hg emissions of anthropogenic origin [19]. In addition, due to anthropogenic warming and nutrient releases, tropical waters have experienced increased oxygen-depletion events [20], conditions that promote the formation of MeHg, and hence the contamination of marine organisms [21–24]. Tropical waters may therefore represent hotspot regions of Hg contamination in biota. Therefore, there is an urgent need to assess Hg contamination and its spatial variations in tropical biota, to better understand the threat posed by environmental Hg loads in these key marine ecosystems.

When monitoring Hg distribution at large spatial scale, the use of bioindicator species is critical [14,25]. Bioindicator organisms reflect the bioavailability of MeHg, which is generated and made available to marine food webs [26]. The Article 19 of the Minamata Convention on Mercury has defined ecological health bioindicators, which includes fish, sea turtles, marine mammals and seabirds. Seabirds are meso- to top predators that integrate and reflect potential Hg contamination of the marine food webs on which they rely [27–29]. As they exhibit large geographical distributions, they permit Hg monitoring across large geographical (both latitudinal and longitudinal) scales (*e.g.*, [30–32]). Considering their significant biomass in all oceans [33,34], their usual colonial nesting and high-site fidelity, numerous individuals can be sampled simultaneously and repeatedly over time [35]. In seabirds, feathers represent a reliable and non-destructive tissue to investigate potential Hg contamination at large spatial scales [36]. Indeed, dietary MeHg accumulates in the body between two moulting episodes [37], 70–90 % of which is then transferred into growing feathers during each moult [38,39]. Furthermore, MeHg has a strong affinity for keratin proteins, the dominant component of feathers, making their bond very stable and withstanding any treatment [40,41]. Although Hg concentrations may vary among different feather types [42,43], they represent a valuable tool for Hg biomonitoring across ocean basins.

In this context, the present study aims to document the spatio-temporal variation in Hg contamination in oceanic ecosystems at the pantropical scale. We selected the sooty tern (*Onychoprion fuscatus*), the most abundant pantropical seabird (18–23 millions of breeding pairs; [44]), as a bioindicator species. First, we investigated large spatial variation by quantifying Hg concentrations in the ventral feathers of sooty terns across 28 colonies, distributed in three ocean basins (*i.e.*, the Pacific, Atlantic and Indian Oceans). Secondly, we compared annual and short-term (*i.e.*, during chick-rearing) Hg contamination by analysing adult and chick feathers, respectively. Considering their shorter exposure period, we expected lower Hg concentrations in chick feathers compared to adults [45]. Thirdly, we investigated temporal variation by comparing Hg concentrations measured here to published literature (*i.e.*, concentrations from one or two decades ago). Finally, we investigated the influence of tern feeding ecology by analysing carbon ($\delta^{13}\text{C}$) and nitrogen ($\delta^{15}\text{N}$) stable isotopes (bulk), which are well-known proxies of the feeding habitat (*i.e.*, carbon source) and diet (*i.e.*, trophic position), respectively [46]. Indeed, the diet is the major route of Hg exposure for seabirds [47,48], and accounting for their feeding ecology is crucial when monitoring Hg contamination in biota [49–52]. However, sources of uncertainty are multiple when interpreting isotopic values from bulk tissues [53], and classical isotopic approaches have thus limitations

when considered at such large spatial scale.

One major limitation lies in baseline isotopic values, which can differ substantially within and between ocean basins, due to differences in (i) environmental conditions that shape them (both spatially and temporally) and (ii) the composition and structure of the phytoplankton communities at the base of marine food webs [54,55]. Therefore, the isotopic signature of the same consumer (e.g., a seabird species) feeding in two isotopically contrasted environments (e.g., two ocean basins with different phytoplankton communities) would incorporate two distinct baseline isotopic values. These baseline effects would thus bias the comparison of these values, and hence their ecological interpretation for the consumer. Compound-Specific Stable Isotope Analyses of Amino-Acids (CSIA-AA) cope with these limitations and reduce uncertainty, as they enable the distinction to be made between baseline and trophic effects, which are characterized by different types of AAs [56, 57]. «Source» AAs are AAs that barely enrich from one trophic level to the next (i.e., they do not fractionate) and hence, reflect the $\delta^{15}\text{N}$ signature of primary producers at the base of the food web (e.g., phenylalanine; [53,58]). In contrast, AAs that undergo substantial isotopic enrichment from diet to consumer are called «trophic» AAs (e.g., glutamic acid; [53,58]). Together, they enable the trophic position of consumers to be calculated, accounting for both baseline and trophic effects [59]. In this study, CSIA-AA were performed on a subset of adult individuals, to allow large-scale comparisons of trophic proxies in sooty terns and investigate their interactions with Hg contamination. Through this coordinated effort, we aim to gain critical baseline data for evaluating Hg contamination in poorly researched tropical marine environments and aid the global effort for monitoring and managing this international pollutant.

2. Material and methods

2.1. Feather sampling and preparation

Feathers were collected from 971 sooty terns at 28 colonies, across the Pacific (n = 9), Atlantic (n = 9) and Indian (n = 10) Oceans (Fig. 1, Table S1). Body feathers (ventral feathers) were collected from both adults (n = 564) and large chicks (i.e., feathered or fledging chicks), hereafter referred as chicks (n = 407). Sampled individuals included predominantly free-living birds, but carcasses were also opportunistically sampled in Palmyra Atoll (n = 1), Motu Oa (n = 2), Puerto Rico (n = 16), Tinhosa Grande (n = 1), Desnoeuf Island (n = 5), African Banks (n = 3), Etoile Cay (n = 1) and Rat Island (n = 2).

To eliminate any external contamination, feathers were cleaned with a mixture of chloroform:methanol (2:1), sonicated for three minutes, rinsed twice in methanol and finally oven-dried for 24–48 h at 45°C. For each tern, four feathers were pooled to derive an individual mean value [61,62] and cut with stainless scissors to obtain a homogenous powder to be analysed for both Hg and stable isotopes.

2.2. Mercury analyses

In seabird feathers, MeHg accounts for > 90 % of the total Hg (THg; [63,64]). Thus, we used THg as a relevant proxy of MeHg burden in sooty tern feathers. THg analyses were performed on feather homogenates (0.3–1.8 mg) in duplicate, using an Advanced Mercury Analyzer (Altec AMA 254). When the relative standard deviation (RSD) was < 10%, Hg concentrations were averaged for each sample. When the RSD was > 10%, an additional sample of the homogenate was analysed and the duplicates guaranteeing the lowest RSD were kept for average calculations. Certified reference materials (CRM) were run to validate accuracy measurement (DOLT-5, Fish liver and TORT-3, Lobster

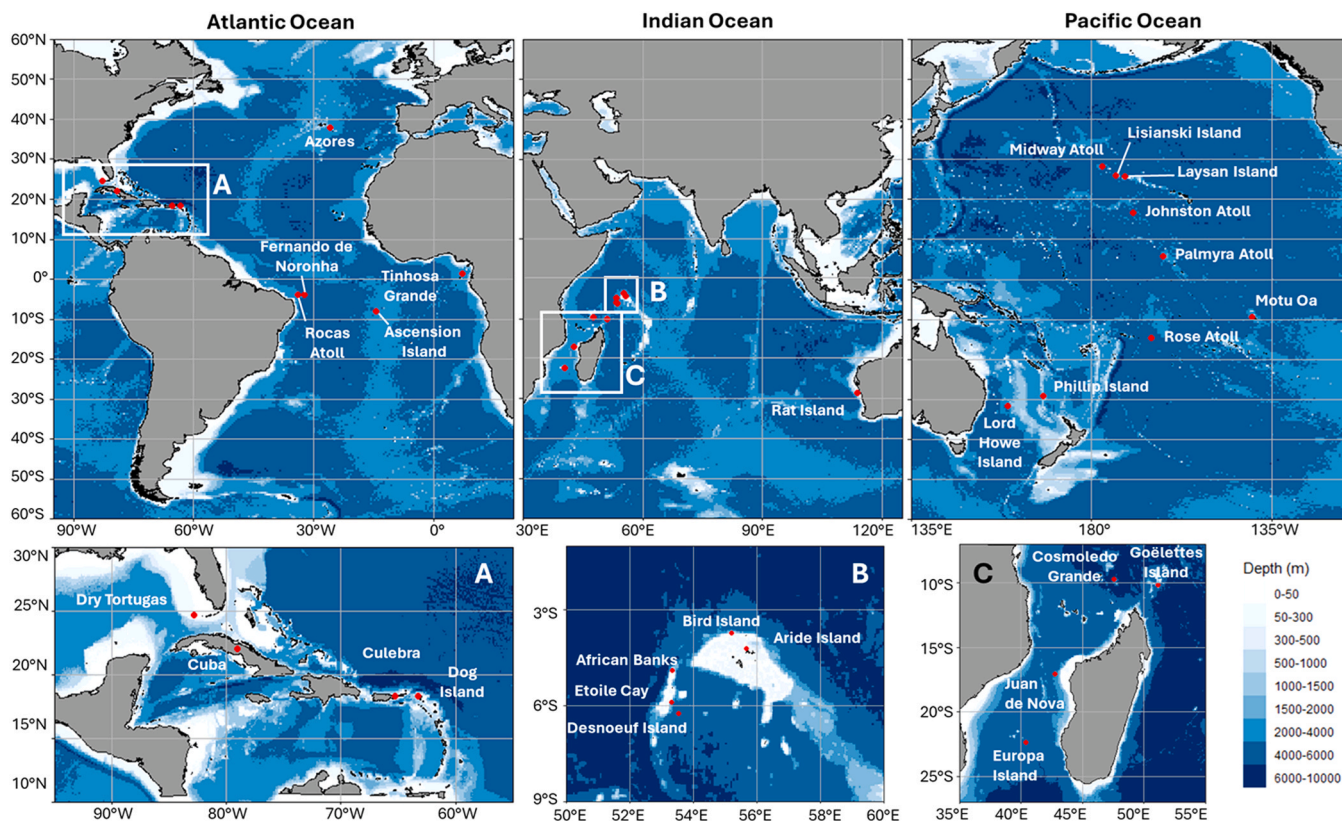


Fig. 1. Spatial distribution of sampled colonies (red dots) of sooty terns (*Onychoprion fuscatus*) across tropical waters, including the Atlantic (n = 9), Indian (n = 10) and Pacific (n = 9) Oceans. The blue gradient indicates bathymetry. Maps were performed with R («ggOceanmaps» package; [60]).

hepatopancreas; National Research Council, Canada; Table S2). CRM recovery values were $96.6 \pm 1.4\%$ and $101.3 \pm 2.4\%$, respectively. Blanks were run at the beginning of each analytical session (*i.e.*, each day). The detection limit of the AMA was 0.1 ng. Mercury concentrations are expressed in $\mu\text{g}\cdot\text{g}^{-1}$ dry weight (dw).

2.3. Bulk stable isotope analyses

Feather homogenates (0.2–0.8 mg) were loaded into tin cups (8 mm \times 5 mm; Elemental Microanalysis Ltd, Okehampton, UK) using a microbalance (XPRUD5, Mettler Toledo, Greifensee, Switzerland), to perform bulk carbon and nitrogen stable isotope analyses. Values of $\delta^{13}\text{C}$ ($^{13}\text{C}/^{12}\text{C}$) and $\delta^{15}\text{N}$ ($^{15}\text{N}/^{14}\text{N}$) were determined with a continuous flow isotope ratio mass spectrometer (Delta V Plus with a ConFlo IV Interface, Thermo Scientific, Bremen, Germany) coupled to an elemental analyzer (Flash 2000 or Flash IRMS EA Isolink CN, Thermo Scientific, Milan, Italy). Results are expressed in the usual δ unit notation relative to Vienna PeeDee Belemnite (V-PDB) for $\delta^{13}\text{C}$ and atmospheric N_2 for $\delta^{15}\text{N}$. Replicate measurements of reference materials (USGS–61 and USGS–63, US Geological Survey) indicated measurement uncertainties $< 0.10\%$ for both $\delta^{13}\text{C}$ and $\delta^{15}\text{N}$ values.

2.4. Compound-specific stable isotope analyses of amino acids (CSIA-AA)

Since CSIA-AA are time- and money-consuming, $\delta^{15}\text{N}$ analyses of phenylalanine (Phe) and glutamic acid (Glu) were performed on a subset of adult individuals ($n = 91$), selected across 19 sites in the three ocean basins (Table S3), representing 68 % of the entire spatial coverage of the study.

Following previously described protocols [65,66], feather homogenates (1.0–1.5 mg) were hydrolysed under nitrogen (200 μL 6 M HCl, 110°C, 22 h). They were then dried under a stream of N_2 at 70°C and finally re-dissolved in 2 mL HCl 0.5 M. Because glutamine (Gln) is converted to Glu during hydrolysis, data for Glu thus represent the total Glu + Gln, noted Glx thereafter. The resultant AAs were purified and derivatized to N-acetyl-isopropyl esters [65]. Norleucine (Alfa Aesar) and alpha-aminoadipic acid (AAA, Sigma-Aldrich) were added as internal standards after AA purification. Caffeine (USGS–61) was added as an internal standard to the derivatized AA before dilution in ethyl acetate for analyses by continuous-flow gas chromatography combustion-isotope ratio mass spectrometry (GC-C-IRMS). $\delta^{15}\text{N}$ values were measured using a Thermo Trace Ultra GC coupled to a Delta Plus isotope-ratio mass spectrometer through a GC Isolink combustion interface (Thermo Scientific, Bremen, Germany). The combustion furnace was maintained at 1000°C, and CO_2 generated during combustion was removed from the carrier gas using a cryogenic trap and released after the end of each analysis. AAs were separated on a TG-624 SilMS column (60 m \times 0.25 mm *i.d.*, 1.4 μm film thickness, Thermo Scientific). Injections were performed in splitless mode (1 min) at 255°C, with a constant helium carrier gas flow (1.2 mL/min). The GC temperature program was set as follows: 70°C (hold 1 min), 165°C at 16 °C/min, 274°C at 4.5 °C/min (hold 22 min), 285°C at 10 °C/min (hold 4 min). Samples were analyzed in duplicates or triplicates. To evaluate drift and accuracy, a standard mixture, thoroughly calibrated by EA-IRMS and derivatized along with the samples, was analysed at the beginning, every three or four samples, and at the end of each batch of analyses. Similar to bulk analyses, data are expressed in delta notation relative to atmospheric N_2 . Raw data were corrected for instrumental variations and deviations in the isotopic compositions of the products occurring during sample derivatization. AA values in the standard mixture were used for correction of any instrumental drift during the run [67] and compound-specific calibration [68]. Precision for AAs $\delta^{15}\text{N}$ values ranged from 0 to 1.5 ‰ (mean 0.3 ‰). Finally, AA derivatives were stored at -20°C until analysis (up to one month).

2.5. Combining feather Hg and stable isotopes

Adult sooty terns start to moult (*i.e.*, basic, post-nuptial moult) while still breeding and replace all of their feathers (flight and body feathers) during the following weeks/months [69]. Body feathers thus reflect Hg exposure since the previous moult, including the breeding and non-breeding periods (*i.e.*, for the past 9–12 months depending on the breeding cycle: sub-annual or annual; [70]). This temporal window also includes a large spatial scale, as adult sooty terns forage primarily in the relative vicinity of their colony during the breeding period (50 to several hundreds of km; [71–74] and can travel thousands of kilometres away from their nesting sites during the non-breeding period. On Ascension Island (South Atlantic Ocean), the non-breeding range of sooty terns averages 2900 km from the colony [75], compared to 4500 km for Bird Island (the Seychelles; [76]). On the other hand, feathers retain the dietary values from the time of their synthesis, as stable isotopes ($\delta^{13}\text{C}$ and $\delta^{15}\text{N}$) are incorporated into feathers as they grow [77]. While Hg and stable isotopes are both incorporated during feather growth, their integration is temporally decoupled [36,78]. Nonetheless, stable isotopes provide essential information about tern feeding ecology and are still relevant to understand the ecological drivers of Hg contamination in adult sooty terns when no other ecological information is available.

In contrast, the temporal mismatch between feather Hg concentrations and stable isotopes is minimal in chicks, as the integration time is almost identical between Hg and stable isotopes in body feathers [79]. Chick feathers thus reflect local Hg exposure (resulting from parents' foraging trips in the vicinity of the colony) during the chick-rearing period [61,80].

2.6. Data analyses

2.6.1. Determining the estimated trophic position of sooty terns

The CSIA-AA method, and more particularly the analysis of $\delta^{15}\text{N}$ values in Glx and Phe, was used to estimate the trophic position (TP) of adult sooty terns during the non-breeding period (see Ohkouchi et al. [53] for a review). Together, source and trophic AAs enable to calculate bird TP from the difference in their $\delta^{15}\text{N}$ values [81,82], with the following formula:

$$\text{TP(feathers)} = 2 + \frac{\delta^{15}\text{NGlx} - \delta^{15}\text{NPhe} - 3.5 \text{ ‰} - 3.4 \text{ ‰}}{6.2 \text{ ‰}} \quad (1)$$

where 6.2 is the overall mean trophic discrimination factor (TDF) across different taxa from McMahon and McCarthy [83], 3.5 is the TDF for gentoo penguin feathers [84] and 3.4 the difference in $\delta^{15}\text{N}$ values between Glx and Phe in primary producers [85].

2.7. Statistical analyses

Statistical analyses and graphical representations were carried out in R 4.2.2 ([86]; «ggplot2» package; [87]), by using two separate datasets: (i) the entire dataset (*i.e.*, with all variables (*i.e.*, Hg and bulk stable isotopes), all sites, both age classes: 564 adults and 407 chicks; hereafter the «global subset»), and (ii) a partial dataset that only included individuals selected for CSIA-AA (adults, $n = 91$) and all variables (*i.e.*, Hg, bulk and compound specific stable isotopes; hereafter the «CSIA subset»). For all statistical analyses, colonies with sample size < 4 were removed (*i.e.*, African Bank, Azores, Etoiles Cay, Laysan Island).

Unifactorial analyses were performed to compare feather Hg concentrations at different spatial scales (between colonies, hemispheres and oceans) in adults and chicks, and between age classes. Hemispheric differences were not tested in the Indian Ocean, because all colonies are located within the Southern Hemisphere. Residual normality and homoscedasticity were examined with Shapiro-Wilk and Breusch-Pagan tests («lmtest» package; [88]), respectively. When test assumptions

were met, a one-way ANOVA and post-hoc Tukey HSD tests were performed to locate the detected differences. Otherwise, non-parametric tests (Kruskal-Wallis and Wilcoxon rank sum tests for multiple and two groups, respectively) were used, followed by a multiple comparisons (Pairwise-Wilcoxon) test when appropriate. Considering the high probability of variation in baseline isotopic values across the three ocean basins (both latitudinally and longitudinally), differences in bulk isotopic values (both $\delta^{13}\text{C}$ and $\delta^{15}\text{N}$ values) were not tested, either at different spatial scales or between age classes. Instead, differences in estimated trophic position (cf. Eq. 1), and $\delta^{15}\text{N}$ values of Glx and Phe were tested on the CSIA subset. Since sooty terns were sampled during two consecutive years in Ascension Island, interannual differences in all variables were also tested in both adults and chicks from this particular site.

Multifactorial analyses were performed to investigate the influence of trophic ecology and colony location on Hg contamination. Prior to the model definition, relationships between continuous variables (*i.e.*, Hg, $\delta^{13}\text{C}$, TP) were tested using a correlation matrix to validate the simultaneous inclusion of non-collinear explanatory variables. Models were Generalized Linear Models (GLMs) with a Gaussian distribution and identity link-function, built using the «nlme» package [89]. For this analysis, we used the CSIA dataset, which included adults only ($n = 88$; colonies with $n > 4$). The initial model was: $\text{Hg} \sim \delta^{13}\text{C} + \text{TP} + \text{Colony}$. Although the variation in baseline $\delta^{13}\text{C}$ values may substantially influence bulk $\delta^{13}\text{C}$ values of sooty tern feathers, bulk $\delta^{13}\text{C}$ values were kept for model selection, as they showed relatively little variation ($-15.9 \pm 0.5 \text{‰}$, $n = 563$). Model selection was based on Akaike's Information Criterion adjusted for small sample sizes (AIC_c). All potential combinations of variables for each dataset are presented in Table 2. Models were ranked using the «dredge» function («MuMIn» package; [90]). Following Burnham and Anderson [91], the model with the lowest AIC_c value and a difference of AIC_c (ΔAIC_c) > 2 when compared with the next best model was considered to be the best. Following Johnson and Omland [92], model performance was assessed using Akaike weights

(w_i). Model assumptions (residual normality, homogeneity, independence) were checked with diagnostic functions («plot» and «qqnorm»). The degree of model fit was reported by using the McFadden's R-Squared metric. Differences between colonies were then identified with Estimated Marginal Means (EMMs; «emmeans» package; [93]) following Bond and Diamond [94]. Finally, partial residuals were extracted from each best model to obtain predictor effect plots («effects» package; [95,96]). This allowed us to control variation in Hg concentrations due to both $\delta^{13}\text{C}$ values and TP to quantify and visualise Hg spatial variation.

3. Results

Feather Hg concentrations (Fig. 2) and bulk stable isotope values (Fig. 3) for the two age classes and all colonies are detailed in Tables 1 and S3, respectively. The AA- $\delta^{15}\text{N}$ values (*i.e.*, Glx and Phe), as well as estimated TP of sooty terns (CSIA subset), are provided in Table S4.

3.1. Age and spatial differences in Hg contamination

Chick terns had lower Hg concentrations than adults (Wilcoxon, $W=189525$, $p < 0.0001$, $n = 965$). In adults (global subset), feather Hg concentrations differed between colonies (Kruskal-Wallis, $\chi^2(23) = 302.1$, $p < 0.0001$, $n = 556$; Fig. 2). When comparing hemispheres within each ocean basin, feather Hg concentrations were higher in the Northern compared to the Southern Hemispheres, both in the Pacific (Wilcoxon, $W=7979$, $p < 0.0001$, $n = 222$) and the Atlantic (Wilcoxon, $W=3833$, $p < 0.001$, $n = 171$) Oceans (Fig. S1). In addition, differences between ocean basins were also found (Kruskal-Wallis, $\chi^2(2) = 47.3$, $p < 0.0001$, $n = 556$), with the highest Hg concentrations in the Atlantic Ocean ($1.36 \pm 0.66 \mu\text{g}\cdot\text{g}^{-1}$, $n = 171$), followed by the Indian ($1.22 \pm 0.29 \mu\text{g}\cdot\text{g}^{-1}$, $n = 195$) and the Pacific ($1.02 \pm 0.48 \mu\text{g}\cdot\text{g}^{-1}$, $n = 197$) Oceans (Fig. S2). Using the CSIA subset, the estimated TP of adult sooty terns was similar between the 18 colonies (ANOVA, $F_{17,70}=1.6$,

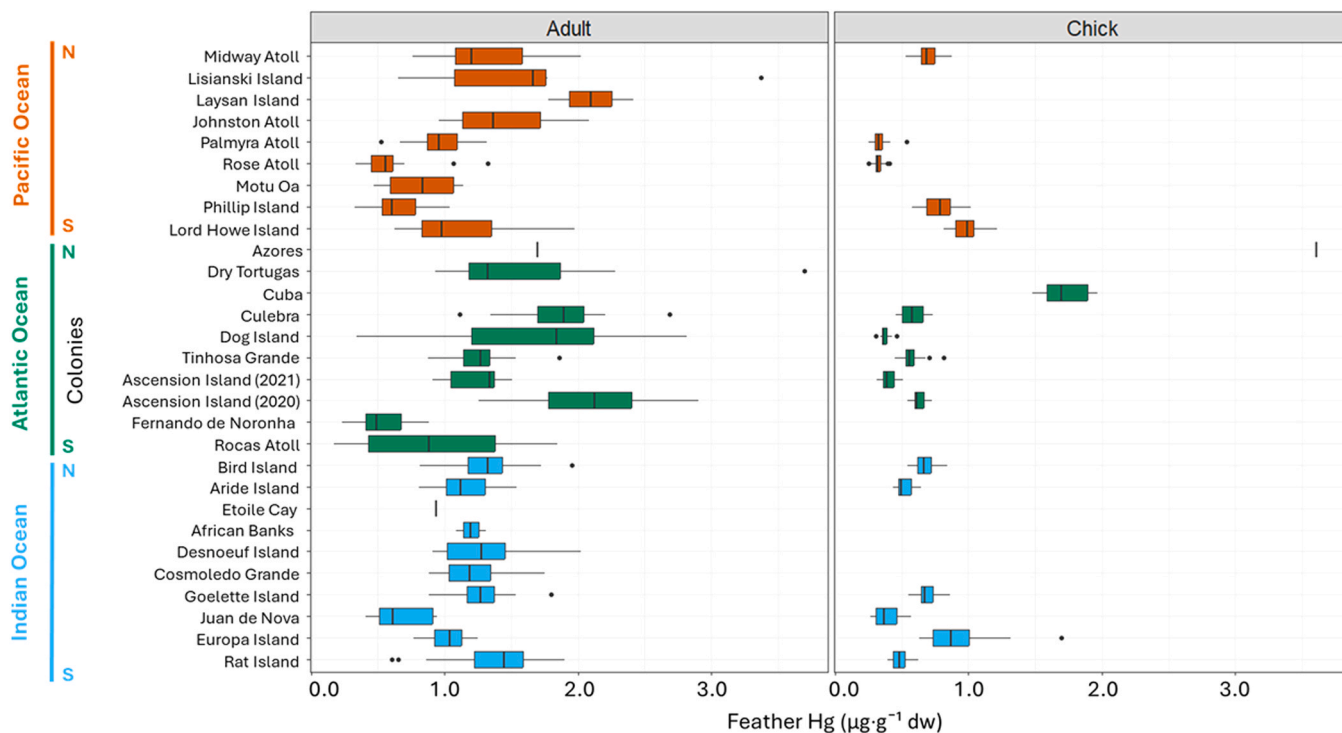


Fig. 2. Feather total Hg concentrations ($\mu\text{g}\cdot\text{g}^{-1}$ dw) in adults (left) and chicks (right) of sooty terns (*Onychoprion fuscatus*), sampled in 28 colonies over three ocean basins. Colonies are ordered from north (N) to south (S) for each ocean basin. Sample sizes are indicated in Table 1. Two consecutive years were sampled in Ascension Island (indicated in brackets). Cuba refers to Felipe de Barlovento and Paredón de Lado cays. Boxplots indicate median values (midlines), errors bars (whiskers) and outliers (black dots).

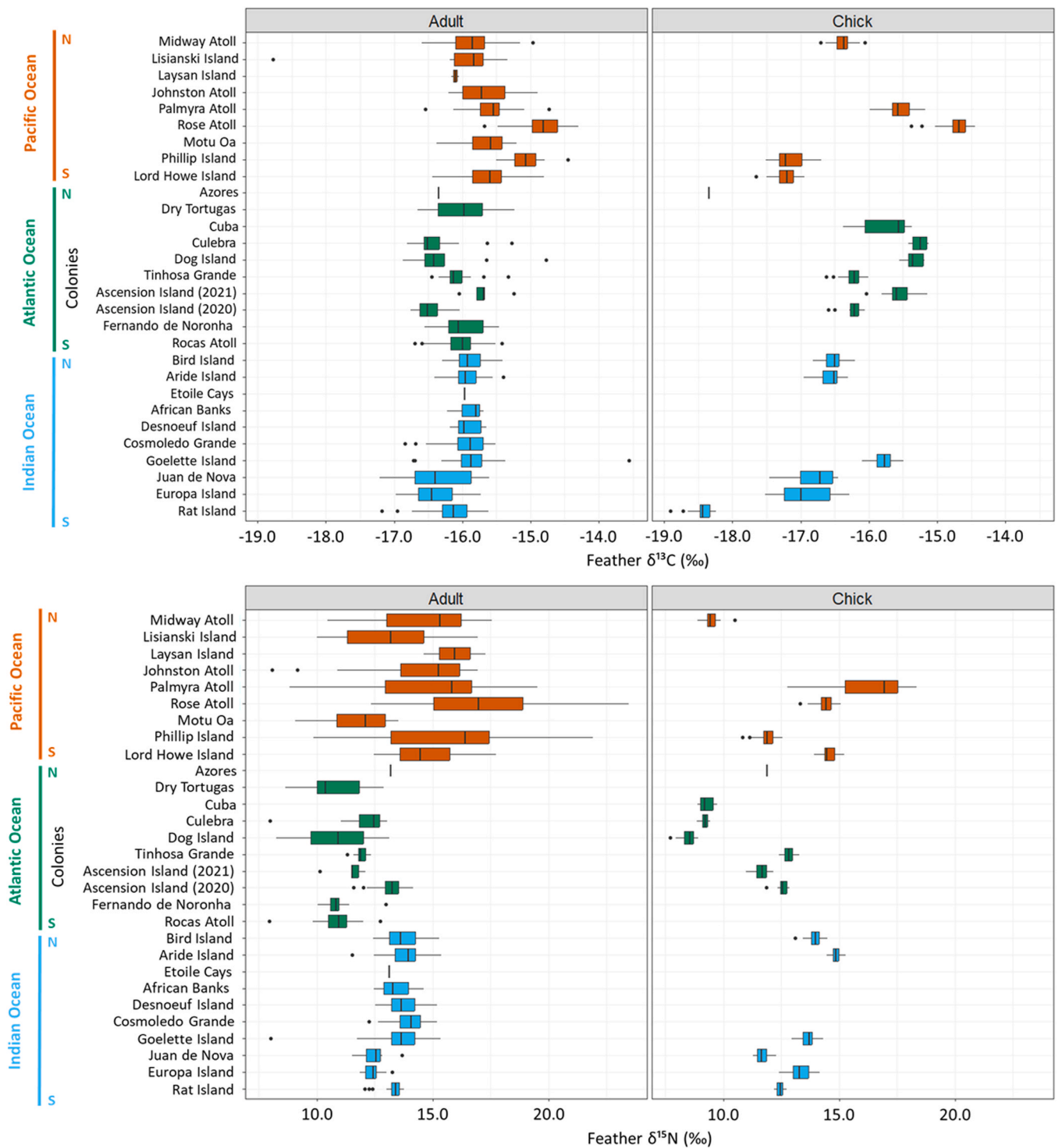


Fig. 3. Feather $\delta^{13}\text{C}$ (top) and $\delta^{15}\text{N}$ (bottom) values (‰) in adults (left) and chicks (right) of sooty terns (*Onychoprion fuscatus*), sampled in 28 colonies over three ocean basins. Colonies are ordered from north (N) to south (S) for each ocean basin. Sample sizes are indicated in Table 1. Two consecutive years were sampled in Ascension Island (indicated in brackets). Cuba refers to Felipe de Barlovento and Paredón de Lado cays. Boxplots indicate median values (midlines), errors bars (whiskers) and outliers (black dots).

$p = 0.09$; Fig. S3.F), but differed across ocean basins (ANOVA, $F_{2,85}=6.7$, $p = 0.002$; Fig. S4). Indeed, TP was significantly lower in the Atlantic Ocean (3.5 ± 0.2 ‰, $n = 35$) compared to the Indian (3.8 ± 0.3 ‰, $n = 20$) and Pacific (3.7 ± 0.3 ‰, $n = 36$) Oceans (Fig. S4.B).

In chicks (global subset), feather Hg concentrations varied among colonies (Kruskal-Wallis, $\chi^2(16) = 338.7$, $p < 0.0001$, $n = 402$; Fig. 2). They also differed between ocean basins (Kruskal-Wallis, $\chi^2(2) = 16.6$,

$p = 0.0003$, $n = 401$), with the Atlantic Ocean ($0.57 \pm 0.33 \mu\text{g}\cdot\text{g}^{-1}$, $n = 93$; lowest concentrations) differing from the Indian Ocean ($0.64 \pm 0.20 \mu\text{g}\cdot\text{g}^{-1}$, $n = 159$; highest concentrations), and the Pacific Ocean ($0.61 \pm 0.28 \mu\text{g}\cdot\text{g}^{-1}$, $n = 149$; Fig. S2). When comparing hemispheres, chick feather Hg concentrations were significantly higher in the South than in the North-Pacific Ocean (Wilcoxon, $W=1604$, $p=0.0001$, $n = 124$; Fig. S1). In contrast, no difference was detected between

Table 1

Literature review of feather Hg concentrations of sooty terns (*Onychoprion fuscatus*) sampled across three ocean basins. See Fig. 1 for the spatial distribution of the sampled colonies, and Table S1 for geographical coordinates. Values are mean \pm SD (min–max).

Sites	Year	Stage	n	Feather Hg ($\mu\text{g}\cdot\text{g dw}$)	References
<u>Pacific Ocean</u>					
Midway Atoll	1990s	Adult	28	1.04 \pm 0.09	[97,98]
	2021	Adult	30	1.30 \pm 0.38 (0.76–2.03)	This study
Lisianski Island	2021	Chick	30	0.70 \pm 0.08 (0.53–0.87)	This study
	2021	Adult	6	1.67 \pm 0.95 (0.66–3.37)	This study
Laysan Island	2021	Adult	2	2.10 \pm 0.45 (1.78–2.42)	This study
Hawaii	1990s	Adult	26	1.26 \pm 0.34	[97]
	1990	Adult	20	0.77 \pm 0.07	[99]
Johnston Atoll	1990	Adult	12	0.98 \pm 0.15	[99]
	2021	Adult	30	1.44 \pm 0.35 (0.96–2.08)	This study
Palmyra Atoll	2021	Adult	31	0.97 \pm 0.05 (0.52–1.32)	This study
	2021	Chick	30	0.33 \pm 0.05 (0.25–0.54)	This study
Rose Atoll	2021	Adult	34	0.57 \pm 0.19 (0.33–1.33)	This study
	2021	Chick	34	0.33 \pm 0.03 (0.25–0.41)	This study
Motu Oa, Ua Pou	2021/2022	Adult	4	0.82 \pm 0.32 (0.47–1.14)	This study
Great Barrier Reef, Michaelmas Cay	1984	Adult	15	0.44 \pm 0.18	[100]
Phillip Island, Norfolk Islands	2020	Adult	30	0.63 \pm 0.19 (0.32–1.04)	This study
	2021	Chick	30	0.78 \pm 0.11 (0.58–1.02)	This study
Lord Howe Island	2020	Adult	30	1.11 \pm 0.39 (0.62–1.97)	This study
	2020	Chick	30	0.98 \pm 0.12 (0.82–1.22)	This study
<u>Atlantic Ocean</u>					
Azores	2021	Adult	1	1.69	This study
	2020	Chick	1	3.61	This study
Dry Tortugas, Florida	2021	Adult	24	1.56 \pm 0.61 (0.93–3.70)	This study
Felipe de Barlovento and Paredón de Lado cays, Cuba	2021	Chick	6	1.72 \pm 0.20 (1.48–1.96)	This study
	1980s	Adult	15	2.64 \pm 0.31	[100]
Culebra, Puerto Rico	2021	Adult	12	1.87 \pm 0.40 (1.12–2.68)	This study
	2021	Chick	4	0.59 \pm 0.12 (0.46–0.73)	This study
Dog Island, Anguilla	2021	Adult	11	1.63 \pm 0.76 (0.34–2.82)	This study
	2021	Chick	13	0.37 \pm 0.04 (0.30–0.46)	This study
Tinhosa Grande	2021	Adult	27	1.27 \pm 0.19 (0.87–1.86)	This study
	2021	Chick	25	0.58 \pm 0.08 (0.45–0.82)	This study
Fernando de Noronha	2011	Adult	18	0.54 \pm 0.18 (0.23–0.89)	This study
Rocas Atoll	2010	Adult	44	0.95 \pm 0.53 (0.17–1.84)	This study
Ascension Island	2020	Adult	5	1.24 \pm 0.25 (0.91–1.51)	This study
	2020	Chick	30	0.40 \pm 0.05 (0.31–0.51)	This study
	2021	Adult	30	2.09 \pm 0.40 (1.25–2.90)	This study
2021	Chick	15	0.63 \pm 0.05 (0.54–0.72)	This study	
<u>Indian Ocean</u>					
Bird Island	2004	Adult	37	0.18 \pm 0.07 (0.10–0.33)	[101]
	2021	Adult	31	1.31 \pm 0.23 (0.82–1.96)	This study
	2021	Chick	33	0.67 \pm 0.06 (0.54–0.84)	This study
Aride Island	1997	Adult	15	1.16 \pm 0.19	[102]
	2003	Adult	14	1.40 \pm 0.49	[102]
	2005	Adult	10	0.59 \pm 0.04	[102]
	2005	Adult	10	0.59 \pm 0.60	[103]
	2021	Adult	30	1.16 \pm 0.19 (0.81–1.54)	This study
	2021	Chick	25	0.52 \pm 0.06 (0.43–0.64)	This study
Etoile Cay	2021	Adult	1	0.94	This study
African Banks	2021	Adult	3	1.20 \pm 0.11 (1.09–1.31)	This study
Desnoeuf Island	2021	Adult	10	1.31 \pm 0.37 (0.91–2.02)	This study
Cosmoledo Grande	2021	Adult	30	1.24 \pm 0.26 (0.89–1.75)	This study
Goëlettes Island	2021	Adult	30	1.28 \pm 0.19 (0.88–1.80)	This study
	2021	Chick	30	0.69 \pm 0.07 (0.55–0.86)	This study
Lys Island, Glorieuses	2004	Adult	14	0.23 \pm 0.10 (0.09–0.39)	[101,103]
	2004	Chick	22	0.05 \pm 0.03 (0.02–0.17)	[101,103]
Europa Island	2003	Adult	18	1.02 \pm 0.15 (0.77–1.25)	This study
	2004	Adult	32	0.21 \pm 0.08 (0.05–0.47)	[101,103]
	2003	Chick	15	0.77 \pm 0.14 (0.63–1.01)	This study
	2021	Chick	16	1.03 \pm 0.24 (0.76–1.69)	This study
Juan de Nova	2003	Adult	10	0.68 \pm 0.22 (0.41–0.94)	This study
	2004	Adult	14	0.39 \pm 0.15 (0.16–0.67)	[101,103]
	2003	Chick	10	0.39 \pm 0.10 (0.27–0.57)	This study
Rat Island, Houtman Abrolhos	2020	Adult	32	1.38 \pm 0.33 (0.61–1.90)	This study
	2020	Chick	30	0.49 \pm 0.06 (0.39–0.62)	This study

hemispheres in the Atlantic Ocean (Wilcoxon, $W=758$, $p = 0.68$, $n = 94$; Fig. S1).

3.2. Interannual differences in Ascension Island

When comparing 2020 and 2021 samples in adults (*i.e.*, global

subset), statistical differences were found for feather Hg concentrations (ANOVA, $F_{1,33}=20.7$, $p = 0.001$; Fig. 4.A), bulk $\delta^{13}\text{C}$ (ANOVA, $F_{1,33}=59.7$, $p < 0.001$; Fig. 4.B) and $\delta^{15}\text{N}$ values (ANOVA, $F_{1,33}=30.7$, $p < 0.001$; Fig. 4.C). For the CSIA subset, there was no significant difference in TP (ANOVA, $F_{1,8}=0.2$, $p = 0.7$; Fig. 4.D) nor in $\delta^{15}\text{N}$ values of Glx (ANOVA, $F_{1,8}=1.2$, $p = 0.3$; Fig. 4.E) across the two sampling years.

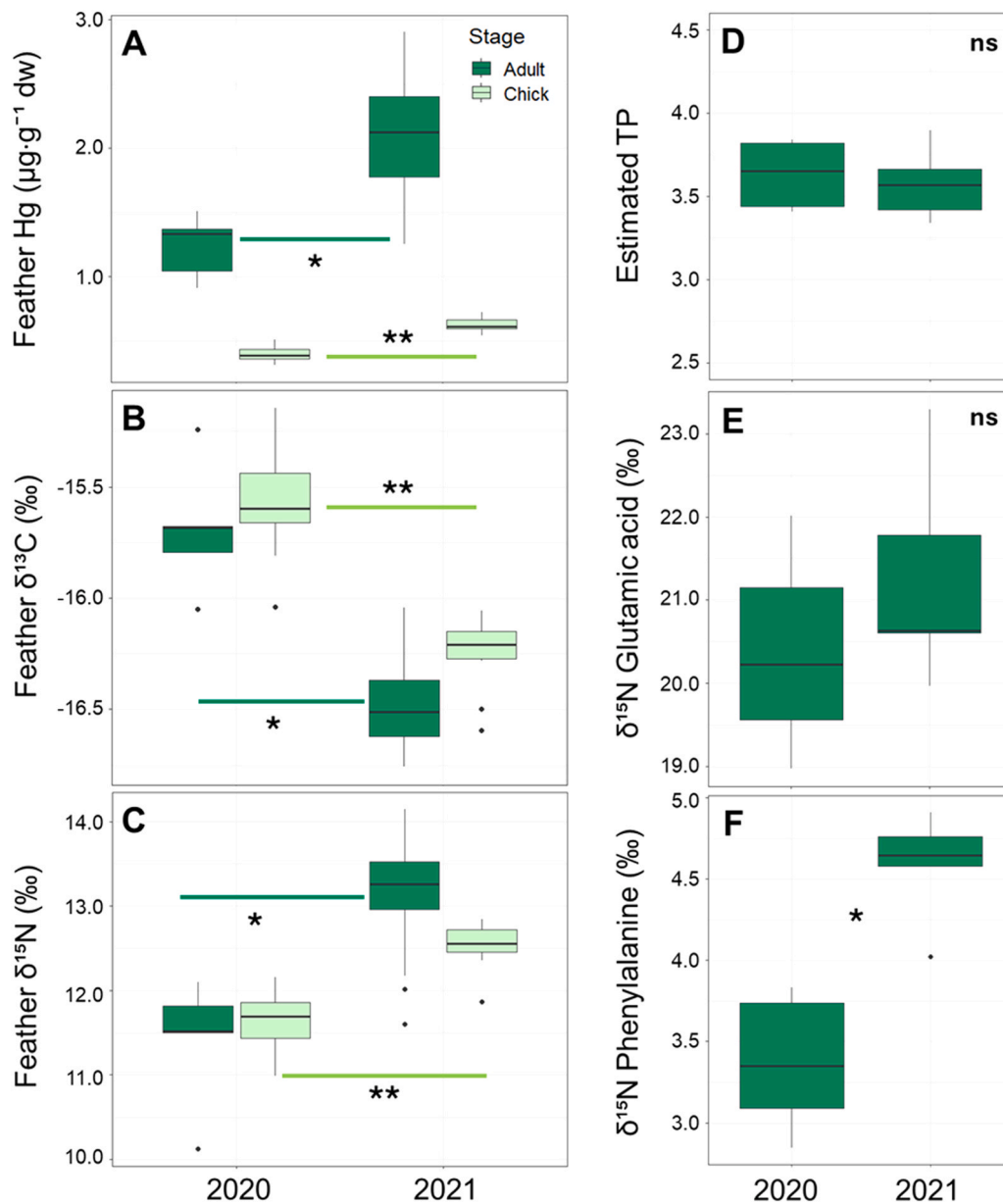


Fig. 4. Interannual differences in feather (A) Hg concentrations ($\mu\text{g}\cdot\text{g}^{-1}\text{ dw}$), (B) bulk $\delta^{13}\text{C}$ and (C) $\delta^{15}\text{N}$ values (‰) of adults ($n = 5$ and $n = 30$ in 2020 and 2021, respectively) and chicks ($n = 30$ and $n = 15$ in 2020 and 2021, respectively) of sooty terns (*Onychoprion fuscatus*), sampled on Ascension Island (South Atlantic Ocean). For a subset of adults ($n = 5$ per year), the (D) trophic position (TP) was estimated with the $\delta^{15}\text{N}$ values of (E) glutamic acid (trophic amino acid) and (F) phenylalanine (source amino acid). Statistical differences between years are indicated when existing, for adults (*) and chicks (**). ns is indicated when no significant difference was detected. Boxplots indicate median values (midlines), errors bars (whiskers) and outliers (black dots).

In contrast, $\delta^{15}\text{N}$ values of Phe differed significantly between 2020 and 2021 (ANOVA, $F_{1,8}=25.4$, $p = 0.001$; Fig. 4.F).

In chicks (*i.e.*, global subset), statistical differences were detected between both years for feather Hg concentrations (ANOVA, $F_{1,43}=1.87.1$, $p < 0.001$; Fig. 4.A), bulk $\delta^{13}\text{C}$ (ANOVA, $F_{1,43}=155.9$, $p < 0.001$; Fig. 4.B) and $\delta^{15}\text{N}$ values (ANOVA, $F_{1,43}=107.2$, $p < 0.001$; Fig. 4.C).

3.3. Influence of trophic ecology on Hg concentrations

Results from model selections performed on the CSIA subset are presented in Table 2. The best model included bulk $\delta^{13}\text{C}$ values and the colony as significant predictors, and explained 68% of the observed variation in feather Hg concentrations (Table 3). Feather Hg concentrations decreased with increasing $\delta^{13}\text{C}$ values (Table 3; Fig. S5). When

Table 2

AICc model ranking from statistical analyses of feather Hg concentrations from sooty terns ($n = 88$). Models are Generalized Linear Models (GLMs) with Gamma distribution, and identity link-function. Abbreviations: k, number of parameters; AICc, Akaike's Information Criterion adjusted for small sample size; w_i AICc weights. A model with $\Delta\text{AIC}_c = 0$ is interpreted as the best model among all the selected ones (in bold). Weights are cumulative (sum to 1).

Models	k	AIC _c	ΔAIC_c	w_i
Hg ~ C + Colony	21	101.6	0.00	0.85
Hg ~ C + Colony + TP	22	105.1	3.47	0.15
Hg ~ C	3	121.5	19.86	0.00
Hg ~ C + TP	4	123.6	21.90	0.00
Hg ~ Colony	20	138.8	37.11	0.00
Hg ~ Colony + TP	21	140.0	38.36	0.00
NULL	2	158.0	56.39	0.00
Hg ~ TP	3	160.2	58.53	0.00

Table 3

Estimated parameters of variables included in the best model ($n = 88$). The model is a Generalized Linear Model (GLM) with Gamma distribution and identity link-function. McFadden's R^2 indicates the degree of model fit (*i.e.*, from low and high model fit indicated from 0 to 1, respectively). Bulk carbon ($\delta^{13}C$) values are proxies of the feeding habitat. The «+» symbol indicates that the colony (categorical factor) is included in the best model. Results for site comparisons (estimated marginal means) are provided in Fig. S6. Abbreviations: CI, confidence interval (95 %); SE, standard error.

Variables	Estimates [CI] \pm SE
Intercept	-7.28 [-9.74, -4.76] \pm 1.22
$\delta^{13}C$	-0.53 [-0.68, -0.37] \pm 0.08
Colony	+
McFadden's R^2	0.68

accounting for $\delta^{13}C$, the colony effect plot showed that: (i) most colonies (61%) exhibited feather Hg concentrations close to the species' average (*i.e.*, $1.19 \mu\text{g}\cdot\text{g}^{-1}$; all colonies combined); (ii) most colonies (75 %) in the Atlantic Ocean had Hg concentrations above this average values, but Fernando de Noronha had three times lower Hg concentrations; (iii) all colonies in the Indian Ocean were below the average, with Juan de Nova and Europa having two times lower Hg concentrations than the other colonies (Fig. 5). These results are reinforced by the EMMs (Fig. S6).

4. Discussion

Using sooty terns as bioindicators of Hg contamination in tropical oceans, the present study provides a unique pantropical assessment of biotic Hg across 28 colonies distributed in three ocean basins, and thereby new information on the bioavailability of MeHg in tropical marine food webs.

4.1. Spatial patterns of Hg contamination in tropical marine food webs

Overall, feather Hg concentrations measured here in adults ($1.19 \mu\text{g}\cdot\text{g}^{-1}$; all sites combined) were similar to those reported in the literature for sooty terns (Table 1) and other tropical sternids at similar locations, such as the brown noddy (*Anous stolidus*; $1.11 \mu\text{g}\cdot\text{g}^{-1}$; [97–99, 101,104,105]), bridled tern (*Onychoprion anaethetus*; $1.36 \mu\text{g}\cdot\text{g}^{-1}$; [100, 105]) and roseate tern (*Sterna dougalii*; $1.57 \mu\text{g}\cdot\text{g}^{-1}$; [100,106]). These low Hg concentrations in body feathers aligns with the feeding ecology of sooty terns, which largely rely on a diet of small epipelagic fish and invertebrates found in surface waters [69,103,107], which have lower Hg concentrations than other mesopelagic and benthic prey species [108–110].

In adult sooty terns, Hg measured in feathers reflects both local contamination during the breeding season and remote contamination during the non-breeding period, resulting in a year-round exposure to Hg over a large spatial oceanic area. Our pantropical sampling of sooty tern feathers allowed a comprehensive comparison of year-round Hg contamination across colonies, both between and within ocean basins (Fig. 2). At the global scale, feather Hg concentrations decreased as followed: Atlantic Ocean > Indian Ocean > Pacific Ocean (Fig. S2). This result coincides with similar findings for the Bulwer's petrel (*Bulweria bulwerii*), a mesopelagic seabird that occupies similar tropical and subtropical regions to sooty terns [32]. Clearly, this highlights existing spatial disparities in Hg distribution at the pantropical scale, between ocean basins, but also between hemispheres within each ocean basin (Fig. S2). Indeed, the Atlantic and Pacific Oceans showed great variability between colonies (Fig. 2). In both oceans, feather Hg concentrations were higher in the northern hemisphere (NH) than in the SH (Fig. S1). This result is consistent with spatial disparities in historical Hg emissions globally. Indeed, Hg emissions have been more prevalent in the NH compared to the SH and tropics [111], mainly for two reasons:

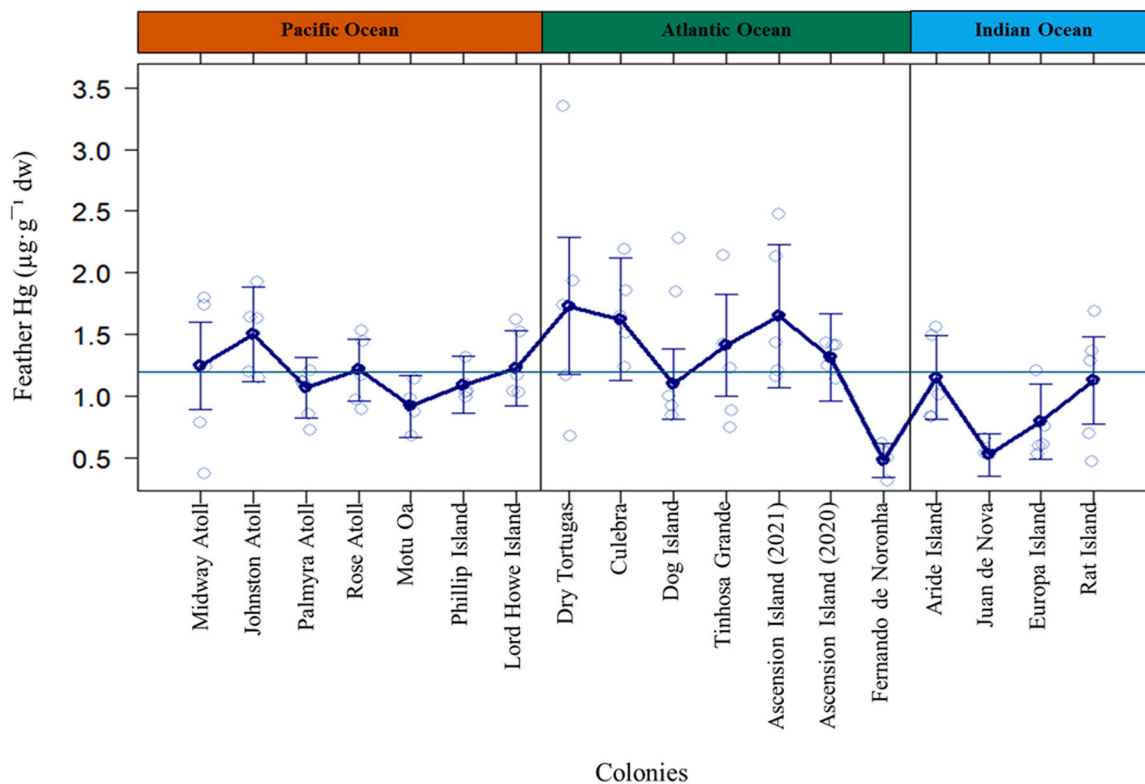


Fig. 5. Spatial differences in feather Hg concentrations ($\mu\text{g}\cdot\text{g}^{-1}$ dw) in adult sooty terns (*Onychoprion fuscaeus*) from 18 tropical colonies ($n = 88$) when controlled by their feeding ecology (feather bulk $\delta^{13}C$ values). Relationships result from the extraction of partial residuals of the best Generalized Linear Model (GLM; see Table 2 and Material and Methods for further details). Individual data are represented in light blue (open circle). Points (filled circle) are means \pm SD. The dark blue line links all mean Hg concentrations. The horizontal line (in blue) represents the species' average (*i.e.*, $1.19 \mu\text{g}\cdot\text{g}^{-1}$).

(1) more historical use of Hg (*i.e.*, 86% of all Hg produced between 1500 and 1900 originated from the NH; [112]), and (2) more industrial activities and related consumption of Hg (*i.e.*, 4-fold larger deposition in the NH than in the SH; [113]). Recent findings demonstrated that such hemispheric differences persist in various environmental compartments of the Pacific Ocean (*i.e.*, atmosphere, seawater, sediments and tunas), where Hg concentrations were systematically higher in the NH ([114, 115] and references therein). More specifically, Médiéu et al. [114] investigated large-scale Hg distribution using skipjack tuna (*Katsuwonus pelamis*) as a bioindicator for the entire Pacific Ocean. They revealed an east-to-west gradient in Hg concentrations, with a Hg hotspot near Asia that was attributed to elevated atmospheric and/or river Hg inputs to coastal waters in the region [116]. These large spatial differences were explained by Hg concentrations in seawater at the base of food webs and inorganic Hg depositions, which vary among different oceanic regions. Unfortunately, our results did not allow to confirm this spatial gradient, considering the lack of feather sampling in South-East Asia (*e.g.*, Indonesia, Philippines, Papua New Guinea), where sooty terns are thought to be abundantly distributed [44]. Yet, within the SH, 15–30% of the total use of Hg in gold-mining occurs in this specific region [111]. Therefore, samples from additional colonies in South-East Asia would substantially improve the present spatial Hg assessment and could help to identify anthropogenic Hg hotspots.

The feathers of chicks reflect local contamination from prey captured by parents around the colony and a short exposure time [35]. As might be expected from their young age and shorter exposure to Hg than adults, mean Hg concentrations in chick feathers were two times lower than in adults ($0.62 \mu\text{g}\cdot\text{g}^{-1}$ vs. $1.19 \mu\text{g}\cdot\text{g}^{-1}$, respectively). Overall, chick Hg concentrations were relatively homogenous across ocean basins, except for two areas that exhibited the highest Hg concentrations: the Azores ($3.61 \mu\text{g}\cdot\text{g}^{-1}$) and Cuba ($1.72 \mu\text{g}\cdot\text{g}^{-1}$). The unique sample in Azores prevents any conclusions to be drawn on the contamination level in this region, which has two interesting characteristics: (i) it exhibits hydrothermal activity [117], and (ii) its seafloor is home to Spanish shipwrecks from the 16th century that likely transported huge quantities of elemental Hg from Europe to the New World [118]. Both could be local sources of Hg in Azores' waters, so further research is required to investigate a potential, local Hg hotspot. Regarding Cuba colonies, feather Hg concentrations were 2.8 times higher than the average for chicks. Interestingly, there is also evidence of feather Hg concentrations being higher than their species' average in other larids breeding at the same colonies, including roseate, royal (*Thalasseus maximus*) and sandwich (*T. sandvicensis*) terns (Garcia-Quintas, unpublished data). This also aligns with previous modelling findings that identified the Caribbean Sea and the Gulf of Mexico among the top 10 coastal oceans which receive high Hg loads from river sources [116]. Clearly, future research in the Caribbean Sea, particularly in Cuba colonies, would help to establish if there is a potential Hg hotspot in these tropical waters, and to further investigate the influence of anthropogenic releases, such as from chlor-alkali plants for example, which likely represent major sources of Hg in this region [119].

4.2. Drivers of Hg contamination and its spatial patterns

In seabirds, trophic ecology is key to understand the mechanisms of Hg exposure and contamination, and to disentangle whether spatial variation in Hg concentrations is related to changes in environmental Hg and/or dietary differences [50,120,121]. In this study, bulk $\delta^{13}\text{C}$ values did not show strong variation across the sampled colonies or ocean basins (Fig. 3), whereas bulk $\delta^{15}\text{N}$ values exhibited high intra- and inter-colony variability, especially in the Pacific Ocean where values ranged from 8.1 to 23.5 ‰ (Table S3). Theoretically, this 15.4 ‰ difference in $\delta^{15}\text{N}$ values would mean a variation of four trophic levels (assuming 3.4 ‰ between each trophic level; [122]), which is unlikely to occur. Thus, this large $\delta^{15}\text{N}$ discrepancy likely indicates strong variation in the baseline isotopic values across the Pacific Ocean, and

prevents the use of bulk $\delta^{15}\text{N}$ values as a reliable proxy of TP in sooty terns at large spatial scale [105]. Using CSIA-AA-derived TP instead, results of model selection revealed that feather Hg concentrations were driven by both bulk $\delta^{13}\text{C}$ values and colony location (68% of variation explained), and not by TP (Table 2). The absence of TP as predictor is consistent with our single bioindicator approach. It is very likely that sooty terns have similar trophic positions across their pantropical distribution range, even though prey species and their corresponding proportions may vary between different oceanic regions and oceans basins. We would expect the opposite result, if studying a more generalist species or several seabird species with distinct trophic ecologies. On the other hand, the presence of bulk $\delta^{13}\text{C}$ values in the predictors suggests that $\delta^{13}\text{C}$ values reflecting the moulting period (*i.e.*, several weeks) partly explain Hg contamination during the inter-moult period (*i.e.*, several months) of adult sooty terns, suggesting that foraging habitat is fairly stable during the non-breeding period. Unlike the Southern Ocean, where the marked latitudinal gradient in $\delta^{13}\text{C}$ values enables the latitudinal tracking of foraging areas of seabirds during the moulting period [123–125], tropical waters are more challenging to study. They are generally devoid of such clear latitudinal variations, as previously shown in the western Indian Ocean [105]. Yet, previous work using stable isotopes clearly identified the Sargassum Sea as wintering grounds for sooty terns breeding on Rocas Atoll (Bugoni et al., unpublished data). Still, without fine-scale tracking of sooty terns' movements within oceanic areas, it is difficult to associate inshore-offshore patterns of their foraging ecology with potential Hg hotspots and coldspots in tropical oceans.

The other predictor of feather Hg concentrations was the colony location, suggesting the role of geographical localization on Hg contamination. Given that Hg concentrations in adult feathers reflect both large spatial and temporal scales, it could be argued that colony location is not the most accurate spatial parameter (*i.e.*, exposure to Hg during the inter-moult period mostly occurs away from the colony). Indeed, trans-hemispheric migration is a common pattern in seabirds [126–128], but even if sooty terns can travel great distances during the non-breeding period, no trans-hemispheric migration was reported yet for this species [75,76]. Therefore, we assumed that they would be relatively constrained regionally around their breeding colonies worldwide. Besides, defining ocean basins as a spatial parameter instead of colonies in the models would imply a substantial loss of spatial information and lead to lower statistical power. Biologging approaches, combined to Hg and stable isotope analyses, could provide further insights into where sooty terns get contaminated by Hg, and investigate whether these areas correspond to different types of foraging habitats in tropical oceans [129].

When accounting for $\delta^{13}\text{C}$ values (which negatively influence feather Hg concentrations; Fig. S5), Hg in feathers across sampled colonies did not show a specific spatial pattern in the Pacific Ocean, with individuals' values varying slightly around the species average (Fig. 5). In the Atlantic Ocean, 71% of the colonies showed higher Hg concentrations than the species average, except for Fernando de Noronha that could represent a Hg coldspot (*i.e.*, low year-round contamination). Because Fernando de Noronha (FdN) is located in the South Atlantic Ocean, approximately 350 km away from Brazil, which represents a major Hg emitter through deforestation of tropical forest and gold-mining [111], one could thus expect the opposite trend. In fact, FdN is very unlikely to be influenced by Amazonian inputs, as the plume spreads northward, because of the circulation of both oceanic currents along the Brazilian coast [130], and atmospheric currents blowing from the east to the west (southeasterly trades). The plausible explanation could be the non-breeding distribution of sooty terns from this colony, which may forage in remote oceanic regions in the central South Atlantic Ocean. Again, biologging approaches would be very useful to confirm this hypothesis in the future. In the Indian Ocean, Hg concentrations were close to the species' average, except for Juan de Nova and Europa Islands that were lower by 43% and 14%, respectively (Fig. 5). Interestingly,

Fernando de Noronha, Juan de Nova and Europa Islands have one feature in common: unlike all other sites that were sampled between 2020 and 2022, these three sites were sampled in 2010 (Brazil) and 2003 (Mozambic Channel), respectively. Therefore, it is difficult to determine here whether Hg contamination is lower in these two specific oceanic regions due to spatial or temporal variation without any additional, recent years of sampling. However, a previous study on Hg temporal variation in sooty terns from Ascension Island recently showed a 0.4% increase per year over the last 145 years (Cusset et al., 2023c). Thus, we could expect Hg concentrations in these three specific colonies today to be higher than in the 2000s and the 2010s.

Besides the aforementioned study, Hg temporal data are very limited in sooty terns. Here, we compared our results for adult birds sampled in the 2020 s with previous findings from the 1990s and the 2000s, across five colonies (Fig. 6; see corresponding references in Table 1). In three colonies (i.e., Midway and Johnston Atolls, and Bird Island), feather Hg concentrations were higher in the 2020 s than in the 1990s/2000s (by 25%, 47% and 628%, respectively). This result is consistent with Hg temporal trends reported worldwide in seabirds [49,131,132], including in sooty terns and tropical waters [63]. In contrast, in Aride Island (Seychelles), feather Hg concentrations showed no difference between 1997 and 2021, while a 53% decrease was observed in Culebra (Puerto Rico) between the 1980s and 2021. Future research is needed to confirm

whether long-term temporal trends in Hg concentrations exist in sooty terns, and if so, whether they are similar on a pantropical scale.

4.3. Interannual differences in Ascension Island

In Ascension Island, both feather Hg concentrations and bulk $\delta^{15}\text{N}$ values were higher in 2021 than in 2020, for both adults and chicks (Fig. 4.A and C; global subset). Consequently, one hypothesis would be that the higher Hg concentrations in 2021 result from the consumption of higher trophic level prey, and hence from higher TP of sooty terns, both during the inter-moult and chick-rearing periods. However, this is disproved by CSIA-AA, which showed that adult TP was relatively similar across these two years (Fig. 4.D). In fact, $\delta^{15}\text{N}$ values of phenylalanine indicate that isotopic baseline has substantially changed between 2020 and 2021 (Fig. 4.F). This drastic change in $\delta^{15}\text{N}$ baseline resulted in higher Hg concentrations in adult sooty terns in 2021, thus suggesting that environmental factors have influenced the increased bioavailability and transfer of Hg in marine food webs in the South Atlantic Ocean. Still, we cannot exclude the possibility that, despite similar TP between years, the diet of sooty terns consisted of different proportions of prey items [107], resulting in different bioaccumulation of Hg between the two years. This is particularly true in specific cases, such as in Dry Tortugas (Florida, USA), where sooty terns have been

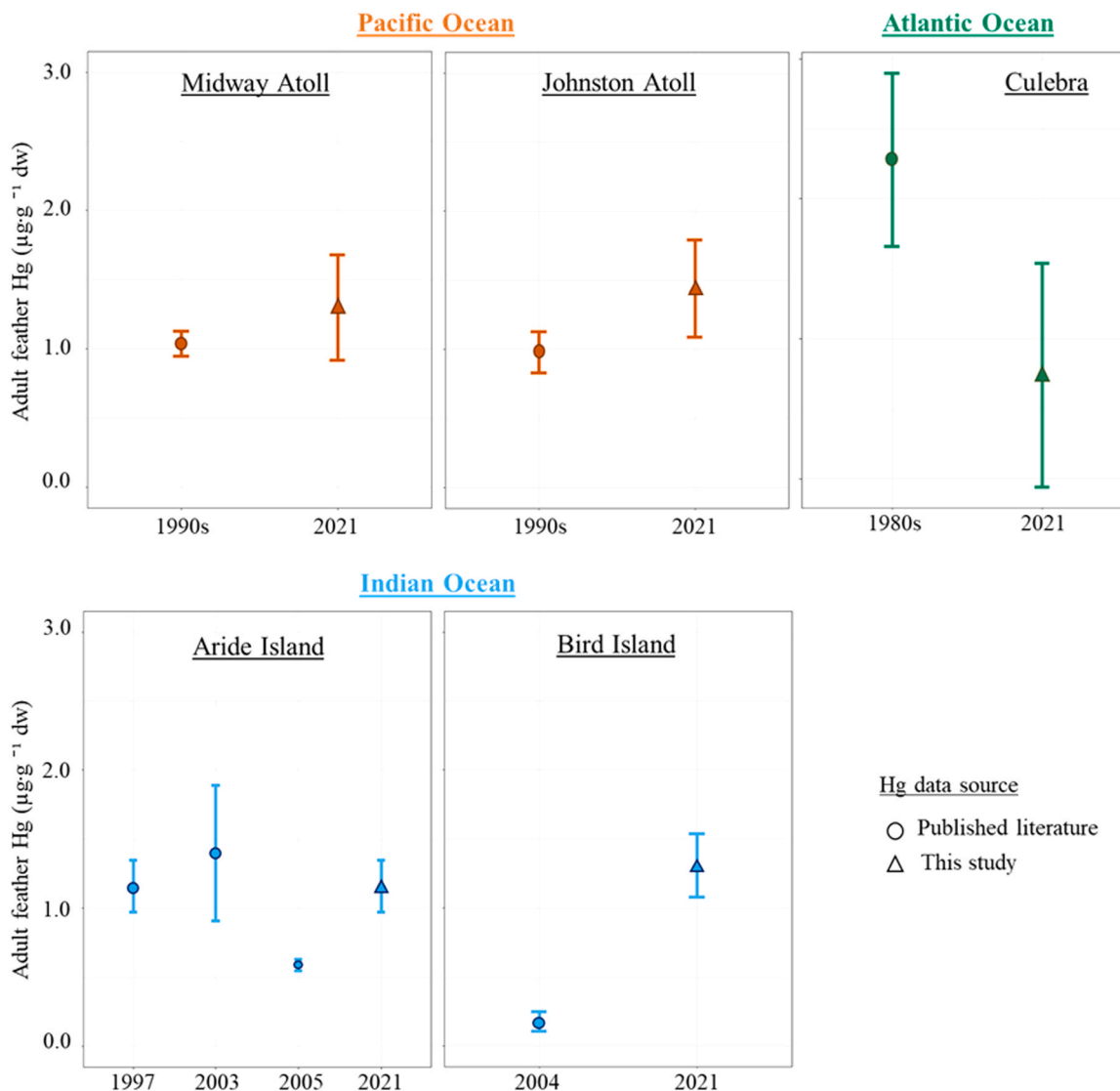


Fig. 6. Temporal comparisons of feather Hg concentrations ($\mu\text{g}\cdot\text{g}^{-1}\text{ dw}$) in adult sooty terns (*Onychoprion fuscatus*) in five colonies across three ocean basins.

observed to consume a wide variety of fish species, including reef-oriented and benthic species brought to the surface by shrimp trawlers [133]. This could only be confirmed by analysing Hg and stable isotopes in the prey species, but obtaining such samples during the non-breeding period of sooty terns is highly challenging, as it implies knowing bird distribution, a missing information.

Similar interannual differences in $\delta^{15}\text{N}$ values of phenylalanine were observed in two previous studies focusing on zooplankton from the Pacific Ocean. The first focused on the North Pacific krill (*Euphausia pacifica*), in the north-western Pacific Ocean [134]. The authors measured a 2.8 ‰ decrease between two consecutive years, characterized by distinct environmental conditions: 1998 with warmer waters, higher stratification and lower chlorophyll a, versus 1999 with abnormally cold, high nutrient waters and high chlorophyll a. This decrease was in fact related to a shift from El Niño (in 1998) to La Niña (in 1999) conditions, which altered nitrogen cycling and associated biogeochemical processes, ultimately impacting $\delta^{15}\text{N}$ values in krill species from the California Current Ecosystem. In sooty terns from Ascension Island, we observed a similar change in $\delta^{15}\text{N}$ values of phenylalanine (1.2 ‰ between 2020 and 2021), and a similar shift from El Niño to La Niña conditions occurred in 2020 (NASA Earth Observatory, 2022). The El Niño Southern Oscillation (ENSO), which is a recurring climate pattern characterized by the succession of El Niño/La Niña phases, has large impacts on the world's climate. It alters the global atmospheric circulation and precipitation system, specifically in subtropical and tropical regions (NASA Earth Observatory, 2022), including the South Atlantic Ocean where Ascension Island is located. The second study focused on several groups of zooplankton in the North Pacific Subtropical Gyre and investigated seasonal variation in $\delta^{15}\text{N}$ values of phenylalanine (winter/summer) during different years ([135], and references therein). Their results also showed a 2 ‰ change between seasons, which was related to seasonal changes in ocean stratification and new production of nitrogen (supported by biological fixation of atmospheric dinitrogen gas and/or entrainment of deep isotopically-enriched nitrates through upwellings; [136,137]). Ultimately, such climate-driven ocean shifts could influence Hg cycling (e.g., Hg depositions, resuspension and bioavailability) in tropical marine ecosystems where sooty terns thrive. For example, upwellings may also act as Hg hotspots, as they can pump Hg-enriched waters from the deep to the surface ocean [138–140]. They could thus enhance Hg bioavailability and accumulation in marine food webs, leading to high Hg concentrations measured in surface marine zooplankton [141,142], which can then be consumed by epipelagic predators such as sooty terns. However, Hg contamination in seabirds results from the combination of a multitude of biogeochemical processes over long periods of time, that are driven by diverse environmental factors, not just the few cited above. Combining diverse environmental factors in future modelling work would be an interesting perspective to further explore the drivers of the pantropical distribution of Hg observed here in sooty terns.

4.4. Conclusions and perspectives

Thanks to a large, field-based scientific network, this study provides a unique assessment of Hg contamination in tropical marine food webs, by using the sooty tern as a pantropical bioindicator species. Overall, the low Hg concentrations in adult and chick sooty terns are consistent with their foraging behaviour and diet, and below the toxicity thresholds recognized for seabird feathers [6]. At the pantropical scale, the highest Hg concentrations were observed in the Atlantic Ocean. At the hemispheric scale, the highest concentrations were measured in the northern hemisphere. Despite the large number of colonies sampled, several regions remain undocumented and clearly deserve further investigations, such as Southeast Asia in the Pacific Ocean, and the central and eastern Indian Ocean. Nonetheless, the present pantropical assessment represents a valuable asset for international Hg biomonitoring programs that aim to protect the environment, wildlife and human populations from

the adverse effects of deleterious contaminants.

Trophic ecology is essential for understanding the drivers involved in Hg contamination and its spatial patterns in marine food webs. However, caution is necessary when interpreting Hg and bulk stable isotope data together. This work provides further evidence of the power of the CSIA-AA approach when considering large spatial scales (among and between ocean basins), and its relevance when combined with Hg monitoring in marine predators, to disentangle the trophic and environmental drivers of Hg contamination in marine food webs. Future investigations of $\delta^{13}\text{C}$ values of AAs represent a valuable, additional tool for further comparisons and more accurate information for both the trophic ecology and ecotoxicology of tropical seabirds. Since Hg contamination was explained by environmental rather than trophic drivers, further research in spatial ecotoxicology is also needed, to identify where exactly sooty terns get contaminated in tropical oceans, and whether this would require adapting local, regional and/or international regulations of anthropogenic Hg emissions.

Beyond spatial variation, Hg contamination in marine food webs results from long-term processes of years, decades or even centuries [2, 18,143,144], that influence the cycling of both natural and anthropogenic Hg in the marine environment, particularly in the context of ongoing climate change [145]. Therefore, renewing such large-scale assessment on a regular basis (e.g., decades) is essential to monitor Hg availability in tropical marine food webs and evaluate the effectiveness of international regulations of Hg, such as the Minamata Convention on Mercury.

Environmental implication

Thanks to a large, field-based scientific network, this study provides a unique assessment of Hg contamination of marine ecosystems, using the sooty tern (*Onychoprion fuscatus*) as pantropical bioindicator species. The highest concentrations were measured in the Northern hemisphere, consistently with higher historical anthropogenic emissions of Hg in the North. Such global assessments are essential to inform international regulatory measures such as the Minamata Convention, and mitigating risks to wildlife and human populations globally. The sooty tern is a highly suitable bioindicator species to monitor the epipelagic domain of tropical oceans in the future.

CRedit authorship contribution statement

Gerard Rocamora: Writing – review & editing, Resources. **Jérôme Fort:** Writing – review & editing, Supervision. **Verónica Costa Neves:** Writing – review & editing, Resources. **Pierre Richard:** Writing – review & editing, Investigation. **Nicholas Carlile:** Writing – review & editing, Resources. **Laura Shearer:** Writing – review & editing, Resources. **Leandro Bugoni:** Writing – review & editing, Resources. **Matthew Morgan:** Writing – review & editing, Resources. **Gaël Guillou:** Writing – review & editing, Investigation. **Patricia Luciano Mancini:** Writing – review & editing, Resources. **Mickaël Charriot:** Writing – review & editing, Investigation. **Terence O'Dwyer:** Writing – review & editing, Resources. **Fanny Cusset:** Writing – review & editing, Writing – original draft, Visualization, Software, Project administration, Methodology, Investigation, Formal analysis, Data curation, Conceptualization. **Yves Chérel:** Writing – review & editing, Supervision, Resources, Conceptualization. **Annabelle Cupidon:** Writing – review & editing, Resources. **Eduardo Ventosa:** Writing – review & editing, Resources. **Antonio Garcia-Quintas:** Writing – review & editing, Resources. **Paco Bustamante:** Writing – review & editing, Supervision, Funding acquisition, Conceptualization. **Nina da Rocha:** Writing – review & editing, Resources.

Declaration of Competing Interest

The authors declare that they have no known competing financial

interests or personal relationships that could have appeared to influence the work reported in this paper.

Acknowledgments

The authors are thankful to all people who contributed to sample collection, preparation and shipment across the 28 colonies of sooty terns. First, we acknowledge the U.S. Fish and Wildlife Service and the activities conducted under National Wildlife Refuge System Special Use Permits in four United States Marine Protected Areas: (i) the Pacific Islands Heritage Marine National Monument (Johnston Atoll National Wildlife Refuge and Palmyra Atoll National Wildlife Refuge; Permit 12543–21002), (ii) the Papahānaumokuākea Marine National Monument (Hawaiian Islands National Wildlife Refuge (Laysan and Lisianski Islands) and Midway Atoll National Wildlife Refuge; permit number: PMNM-2021–014), (iii) Rose Atoll Marine National Monument and National Wildlife Refuge, and (iv) Culebra National Wildlife Refuge (Puerto Rico). Staff from these Monuments and National Wildlife Refuges are acknowledged for their support during permit preparation and sampling organization, namely Kate Toniolo, Daniel Link, Brian Peck and Ana Roman. These activities were conducted in the USA under Migratory Bird Permit Import/Export (N° MBPER0018031). For French Polynesia, we are grateful to the Société Ornithologique de Polynésie MANU for providing feathers from Ua Pou, specifically to Tehani Withers and Thomas Ghestemme. For islands in the Tasman Sea, we acknowledge Emily Mowat (Birdlife Australia) as well as the staff from Parks Australia on Phillip Island and on Lord Howe Island, the staff of the Lord Howe Island Board. Samples were collected under DPE Scientific Licence SL100668 and AEC 021028/02 and permits 2020/R/03 (Parks Australia) and LHIB 07/20 (Lord Howe Island Board).

For bird sampling in Cuba, we acknowledge the ARTS programme of the French Institut de Recherche pour le Développement (IRD), in collaboration with the Centro de Investigaciones de Ecosistemas Costeros (CIEC) of Cuba, which supported the PhD scholarship of Antonio Garcia-Quintas. Thanks also to the Oficina de Regulación y Seguridad Ambiental (ORSA) of Cuba for providing the environmental permits to collect the samples. Thanks are also due to Louise Soanes and Stuart Pimm for providing samples from Dog Island (Anguilla) and Dry Tortugas (Florida, USA), respectively. Sophie Tuppen is acknowledged for assistance during field work on Ascension Island. The work performed in the Azores received national funds through the FCT – Foundation for Science and Technology, I.P., under the project UIDB/05634/2025 and UIDP/05634/2025 and through the Regional Government of the Azores through the project M1.1.A/FUNC.UI&D/003/2021–2024. In São Tomé and Príncipe, we would like to thank Fundação Príncipe for their support in sample collection and in particular Yodiney Santos and Ayres Pedronho for their help on the field, as well as Estrela Matilde for helping with logistics in field work organization. Samples in Brazil were collected through funds provided by Brazilian National Research Council (CNPq, Proc. 557152/09–7) and CAPES Foundation. LB is CNPq Research fellowship (Proc. 310145/2022–8). Sampling permits were granted by ICMBio (No. 22697–4).

For the Seychelles, we acknowledge the following persons and institutions for their support in sample collection: (i) the Island Conservation Society (ICS) with Pierre-André Adam, Mickaél Napoleon, Nicky Jean, Liam Padayachy, Ricky Adeline, Annie Gendron and Dillys Pouponeau, as well as the staff of the Ministry of Agriculture, Climate Change and Environment (MACCE) (Indira Gamatis), and Magali Rocamora (IBC-UniSey) for their assistance in the field; (ii) the Government of Seychelles, MACCE, including Indira Gamatis for helping in the field, and the Seychelles Bureau of Standards (SBS) for granting approval for this research; (iii) the Islands Development Company (IDC), Farquhar, Cosmoledo & Astove, Marie-Louise & Desnoeufs, Rémire & African Banks Foundations for logistical and financial support; and (iv) ICS Head Office Management Team for their support in coordinating and facilitating the administration procedures associated with this project.

Also, we thank Chris Feare for his contribution for Bird Island, where the work was made possible by its owners who have supported research there over many years: Guy Savy and family. Feather sampling was helped by Seychelloise assistants Rachel Bristol and Christine Larose. Thanks to Charles-Andre Bost (CEBC) and Nicholas Dunlop (Conservation Council Western Australia) for providing feathers from Europa (Mozambic Channel), and Abrolhos Islands (Australia), respectively.

Feather samples were shipped from all collaborating countries under appropriate French import permits (N°: FR17201182LR (2020), FR17211006LR (2021), FR17211289LR (2022)).

Regarding laboratory analyses, we are grateful to: (i) Louis Troussé and Margaux Mollier for their help in the laboratory during their internships, and (ii) Carine Churlaud and Maud Brault-Favrou from the Plateforme Analyses Élémentaires (LIENSs) for their support during Hg analyses. Thanks are due to the CPER (Contrat de Projet État-Région) and the FEDER (Fonds Européen de Développement Régional) for funding the AMA and the IRMS of LIENSs laboratory. The IUF (Institut Universitaire de France) is acknowledged for its support to Paco Bustamante as a Senior Member. This work benefitted from the French GDR Aquatic Ecotoxicology framework, that aims to foster stimulating scientific discussions for more integrative approaches. Finally, thanks to Clément Bertin and Julie Charrier for their respective contributions to the graphical abstract (i.e., map and drawing of the sooty tern).

Appendix A. Supporting information

Supplementary data associated with this article can be found in the online version at [doi:10.1016/j.jhazmat.2026.141530](https://doi.org/10.1016/j.jhazmat.2026.141530).

Data availability

Data will be made available on request.

References

- [1] Amos, H.M., Jacob, D.J., Streets, D.G., Sunderland, E.M., 2013. Legacy impacts of all-time anthropogenic emissions on the global mercury cycle. *Glob Biogeochem Cycles* 27, 410–421. <https://doi.org/10.1002/gbc.20040>.
- [2] Driscoll, C.T., Mason, R.P., Chan, H.M., Jacob, D.J., Pirrone, N., 2013. Mercury as a global pollutant: Sources, pathways, and effects. *Environ Sci Technol* 47, 4967–4983. <https://doi.org/10.1021/es305071v>.
- [3] Streets, D.G., Horowitz, H.M., Lu, Z., Levin, L., Thackray, C.P., Sunderland, E.M., 2019. Five hundred years of anthropogenic mercury: Spatial and temporal release profiles. *Environ Res Lett* 14. <https://doi.org/10.1088/1748-9326/ab281f>.
- [4] Driscoll, C.T., Han, Y.-J., Chen, C.Y., Evers, D.C., Lambert, K.F., Holsen, T.M., Kamman, N.C., Munson, R.K., 2007. Mercury contamination in forest and freshwater ecosystems in the Northeastern United States. *BioScience* 57, 17–28. <https://doi.org/10.1641/B570106>.
- [5] Scheuhammer, A.M., Basu, N., Evers, D.C., Heinz, G.H., Sandheinrich, M.B., Bank, M.S., 2012. Ecotoxicology of mercury in fish and wildlife: Recent advances. In: Bank, M. (Ed.), *Mercury in the environment: Pattern and process*. University of California Press, p. 0. <https://doi.org/10.1525/california/9780520271630.003.0011>.
- [6] Chastel, O., Fort, J., Ackerman, J.T., Albert, C., Angelier, F., Basu, N., Blévin, P., Brault-Favrou, M., Bustnes, J.O., Bustamante, P., Danielsen, J., Descamps, S., Dietz, R., Erikstad, K.E., Eulaers, I., Ezhov, A., Fleishman, A.B., Gabrielsen, G.W., Gavrilo, M., Gilchrist, G., Gilg, O., Gíslason, S., Golubova, E., Goutte, A., Grémillet, D., Hallgrímsson, G.T., Hansen, E.S., Hanssen, S.A., Hatch, S., Huffeldt, N.P., Jakubas, D., Jönsson, J.E., Kitaysky, A.S., Kolbeinsson, Y., Krasnov, Y., Letcher, R.J., Linnebjerg, J.F., Mallory, M., Merkel, F.R., Moe, B., Montevecchi, W.J., Mosbech, A., Olsen, B., Orben, R.A., Provencher, J.F., Ragnarsdóttir, S.B., Reiertsen, T.K., Rojek, N., Romano, M., Søndergaard, J., Strøm, H., Takahashi, A., Tartu, S., Thórarinnsson, T.L., Thiebot, J.-B., Will, A.P., Wilson, S., Wojczulanis-Jakubas, K., Yannic, G., 2022. Mercury contamination and potential health risks to Arctic seabirds and shorebirds. *Sci Total Environ*, 156944. <https://doi.org/10.1016/j.scitotenv.2022.156944>.
- [7] Ibañez, A.E., Mills, W.F., Bustamante, P., Morales, L.M., Torres, D.S., D' Astek, B., Mariano-Jelicich, R., Phillips, R.A., Montalti, D., 2024. Deleterious effects of mercury contamination on immunocompetence, liver function and egg volume in an Antarctic seabird. *Chemosphere* 346, 140630. <https://doi.org/10.1016/j.chemosphere.2023.140630>.
- [8] Basu, N., Bastiansz, A., Dóra, J.G., Fujimura, M., Horvat, M., Shroff, E., Weihe, P., Zastenskaya, I., 2023. Our evolved understanding of the human health risks of mercury. *Ambio*. <https://doi.org/10.1007/s13280-023-01831-6>.

- [9] Bertram, J., Bichet, C., Moiron, M., Beccardi, M., Kürten, N., Schupp, P.J., Bouwhuis, S., 2025. Mercury levels in chicks of a long-lived seabird – Parental effects and links with growth and survival. *Environ Res* 285, 122283. <https://doi.org/10.1016/j.envres.2025.122283>.
- [10] De La Peña-Lastra, S., Pérez-Alberti, A., Ferreira, T.O., Huerta-Díaz, M.Á., Otero, X.L., 2022. Global deposition of potentially toxic metals via faecal material in seabird colonies. *Sci Rep* 12, 22392. <https://doi.org/10.1038/s41598-022-26905-5>.
- [11] Obrist, D., Kirk, J.L., Zhang, L., Sunderland, E.M., Jiskra, M., Selin, N.E., 2018. A review of global environmental mercury processes in response to human and natural perturbations: Changes of emissions, climate, and land use. *Ambio* 47, 116–140. <https://doi.org/10.1007/s13280-017-1004-9>.
- [12] Eagles-Smith, C.A., Silbergeld, E.K., Basu, N., Bustamante, P., Diaz-Barriga, F., Hopkins, W.A., Kidd, K.A., Nyland, J.F., 2018. Modulators of mercury risk to wildlife and humans in the context of rapid global change. *Ambio* 47, 170–197. <https://doi.org/10.1007/s13280-017-1011-x>.
- [13] Horowitz, H.M., Jacob, D.J., Zhang, Y., Dibble, T.S., Slemr, F., Amos, H.M., Schmidt, J.A., Corbitt, E.S., Marais, E.A., Sunderland, E.M., 2017. A new mechanism for atmospheric mercury redox chemistry: Implications for the global mercury budget. *Atmos Chem Phys* 17, 6353–6371. <https://doi.org/10.5194/acp-17-6353-2017>.
- [14] Evers, D.C., Ackerman, J.T., Åkerblom, S., Bally, D., Basu, N., Bishop, K., Bodin, N., Braaten, H.F.V., Burton, M.E.H., Bustamante, P., Chen, C., Chételat, J., Christian, L., Dietz, R., Drevnick, P., Eagles-Smith, C., Fernandez, L.E., Hammerschlag, N., Harmelin-Vivien, M., Harte, A., Krümmel, E.M., Brito, J.L., Medina, G., Barrios Rodriguez, C.A., Stenhouse, I., Sunderland, E., Takeuchi, A., Tear, T., Vega, C., Wilson, S., Wu, P., 2024. Global mercury concentrations in biota: Their use as a basis for a global biomonitoring framework. *Ecotoxicology*. <https://doi.org/10.1007/s10646-024-02747-x>.
- [15] Selin, H., Keane, S.E., Wang, S., Selin, N.E., Davis, K., Bally, D., 2018. Linking science and policy to support the implementation of the Minamata Convention on Mercury. *Ambio* 47, 198–215. <https://doi.org/10.1007/s13280-017-1003-x>.
- [16] Chen, C.Y., Driscoll, C.T., Eagles-Smith, C.A., Eckley, C.S., Gay, D.A., Hsu-Kim, H., Keane, S.E., Kirk, J.L., et al., 2018. A critical time for mercury science to inform global policy. *Environ Sci Technol* 52, 9556–9561.
- [17] Chen, C.Y., Evers, D.C., 2023. Global mercury impact synthesis: Processes in the Southern Hemisphere. *Ambio*. <https://doi.org/10.1007/s13280-023-01842-3>.
- [18] UN Environment, 2019. Global Mercury Assessment 2018. UN Environment Programme. Chemicals and Health Branch, Geneva, Switzerland. ISBN: 978-92-807-3744-8.
- [19] Keane, S., Bernaudat, L., Davis, K.J., Stylo, M., Mutemer, N., Singo, P., Twala, P., Mutemer, I., Nakafeero, A., Etui, I.D., 2023. Mercury and artisanal and small-scale gold mining: Review of global use estimates and considerations for promoting mercury-free alternatives. *Ambio*. <https://doi.org/10.1007/s13280-023-01843-2>.
- [20] Breitburg, D., Levin, L.A., Oschlies, A., Grégoire, M., Chavez, F.P., Conley, D.J., Garçon, V., Gilbert, D., Gutiérrez, D., Isensee, K., Jacinto, G.S., Limburg, K.E., Montes, I., Naqvi, S.W.A., Pitcher, G.C., Rabalais, N.N., Roman, M.R., Rose, K.A., Seibel, B.A., Telszewski, M., Yasuhara, M., Zhang, J., 2018. Declining oxygen in the global ocean and coastal waters. *Science* 359, eaam7240. <https://doi.org/10.1126/science.aam7240>.
- [21] Schartup, A.T., Thackray, C.P., Qureshi, A., Dassuncao, C., Gillespie, K., Hanke, A., Sunderland, E.M., 2019. Climate change and overfishing increase neurotoxicant in marine predators. *Nature* 572, 648–650. <https://doi.org/10.1038/s41586-019-1468-9>.
- [22] Sunderland, E.M., Krabbenhoft, D.P., Moreau, J.W., Strode, S.A., Landing, W.M., 2009. Mercury sources, distribution, and bioavailability in the North Pacific Ocean: Insights from data and models. *Glob Biogeochem Cycles* 23. <https://doi.org/10.1029/2008GB003425>.
- [23] Cossa, D., 2013. Methylmercury manufacture. *Nat Geosci* 6, 810–811. <https://doi.org/10.1038/ngeo1967>.
- [24] Mason, R.P., Choi, A.L., Fitzgerald, W.F., Hammerschmidt, C.R., Lamborg, C.H., Soerensen, A.L., Sunderland, E.M., 2012. Mercury biogeochemical cycling in the Ocean and policy implications. *Environ Res* 119, 101–117. <https://doi.org/10.1016/j.envres.2012.03.013>.
- [25] Evers, D.C., Keane, S.E., Basu, N., Buck, D., 2016. Evaluating the effectiveness of the Minamata Convention on Mercury: Principles and recommendations for next steps. *Sci Total Environ* 569–570, 888–903. <https://doi.org/10.1016/j.scitotenv.2016.05.001>.
- [26] Mason, R.P., Abbott, M.L., Bullock, O.R., Driscoll, C.T., Evers, D., Lindberg, S.E., Murray, M., Swain, E.B., 2005. Monitoring the response to changing mercury deposition. *Environ Sci Technol* 39, 14A–22A. <https://doi.org/10.1021/es053155l>.
- [27] Burger, J., Gochfeld, M., 2004. Marine birds as sentinels of environmental pollution. *EcoHealth* 1, 263–274. <https://doi.org/10.1007/s10393-004-0096-4>.
- [28] Furness, R.W., 1993. Birds as monitors of pollutants. In: Furness, R.W., Greenwood, J.J.D. (Eds.), *Birds as Monitors of Environmental Change*. Springer Netherlands, Dordrecht, pp. 86–143. https://doi.org/10.1007/978-94-015-1322-7_3.
- [29] Furness, R.W., Camphuysen, K. (C.J.), 1997. Seabirds as monitors of the marine environment. *ICES J Mar Sci* 54, 726–737. <https://doi.org/10.1006/jmsc.1997.0243>.
- [30] Albert, C., Moe, B., Ström, H., Grémillet, D., Brault-Favrou, M., Tarroux, A., Descamps, S., Bräthen, V.S., Merkel, B., Åström, J., Amélineau, F., Angelier, F., Anker-Nilssen, T., Chastel, O., Christensen-Dalsgaard, S., Danielsen, J., Elliott, K., Erikstad, K.E., Ezhov, A., Fauchald, P., Gabrielsen, G.W., Gavrilov, M., Hanssen, S., Helgason, H.H., Johansen, M.K., Kolbeinsson, Y., Krasnov, Y., Langset, M., Lemaire, J., Lorentsen, S.-H., Olsen, B., Patterson, A., Plumejeaud-Perreau, C., Reiertsen, T.K., Systad, G.H., Thompson, P.M., Lindberg Thórarinnsson, T., Bustamante, P., Fort, J., 2024. Seabirds reveal mercury distribution across the North Atlantic. *Proc Natl Acad Sci* 121, e2315513121. <https://doi.org/10.1073/pnas.2315513121>.
- [31] Cusset, F., Bustamante, P., Carravieri, A., Bertin, C., Brasso, R., Corsi, I., Dunn, M., Emmerson, L., Guillou, G., Hart, T., Juárez, M., Kato, A., Machado-Gaye, A.L., Michelot, C., Olmastroni, S., Polito, M., Raclot, T., Santos, M., Schmidt, A., Southwell, C., Soutullo, A., Takahashi, A., Thiebot, J.-B., Trathan, P., Vivion, P., Waluda, C., Fort, J., Cherel, Y., 2023. Circumpolar assessment of mercury contamination: The Adélie penguin as a bioindicator of Antarctic marine ecosystems. *Ecotoxicology*. <https://doi.org/10.1007/s10646-023-02709-9>.
- [32] Furtado, R., Granadeiro, J.P., Gatt, M.C., Rounds, R., Horikoshi, K., Paiva, V.H., Menezes, D., Pereira, E., Catry, P., 2021. Monitoring of mercury in the mesopelagic domain of the Pacific and Atlantic oceans using body feathers of Bulwer's petrel as a bioindicator. *Sci Total Environ* 775, 145796. <https://doi.org/10.1016/j.scitotenv.2021.145796>.
- [33] Paleczny, M., Karpouzi, V.S., Hammill, E., Pauly, D., 2016. Global seabird populations and their food consumption. Pp. 125–136. In: Pauly, D., Zeller, D. (Eds.), *Global Atlas of Marine Fisheries: A Critical Appraisal of Catches and Ecosystem Impacts*. Island Press, Washington, DC.
- [34] Brooke, M., 2004. The food consumption of the world's seabirds. *Proc R Soc Lond B Biol Sci* 271, S246–S248. <https://doi.org/10.1098/rsbl.2003.0153>.
- [35] Albert, C., Renedo, M., Bustamante, P., Fort, J., 2019. Using blood and feathers to investigate large-scale Hg contamination in Arctic seabirds: A review. *Environ Res* 177, 108588. <https://doi.org/10.1016/j.envres.2019.108588>.
- [36] Thompson, D.R., Bearhop, S., Speakman, J.R., Furness, R.W., 1998. Feathers as a means of monitoring mercury in seabirds: Insights from stable isotope analysis. *Environ Pollut* 101, 193–200. [https://doi.org/10.1016/S0269-7491\(98\)00078-5](https://doi.org/10.1016/S0269-7491(98)00078-5).
- [37] Furness, R.W., Muirhead, S.J., Woodburn, M., 1986. Using bird feathers to measure mercury in the environment: Relationships between mercury content and moult. *Mar Pollut Bull* 17, 27–30. [https://doi.org/10.1016/0025-326X\(86\)90801-5](https://doi.org/10.1016/0025-326X(86)90801-5).
- [38] Honda, K., Nasu, T., Tatsukawa, R., 1986. Seasonal changes in mercury accumulation in the black-eared kite, *Milvus migrans lineatus*. *Environ Pollut Ser Ecol Biol* 42, 325–334. [https://doi.org/10.1016/0143-1471\(86\)90016-4](https://doi.org/10.1016/0143-1471(86)90016-4).
- [39] Williams, K.A., Evers, D.C., 2011. The role of mercury in songbird population declines: Exposure on the wintering grounds and during migration. Permit report to the Florida Department of Environmental Protection, Division of Recreation and Parks. Report BRI 2011-01. BioDiversity Research Institute, Gorham, Maine.
- [40] Appelquist, H., Asbirk, S., Drabæk, I., 1984. Mercury monitoring: Mercury stability in bird feathers. *Mar Pollut Bull* 15, 22–24. [https://doi.org/10.1016/0025-326X\(84\)90419-3](https://doi.org/10.1016/0025-326X(84)90419-3).
- [41] Crewther, W.G., Fraser, R.D., Lennox, F.G., Lindley, H., 1965. The chemistry of keratins. *Adv Protein Chem* 20, 191–346. [https://doi.org/10.1016/s0065-3233\(08\)60390-3](https://doi.org/10.1016/s0065-3233(08)60390-3).
- [42] Bighetti, G.P., Padilha, J.A., Cunha, L.S.T., Malm, O., Mancini, P.L., 2022. Ventral feathers contained the highest mercury level in brown booby (*Sula leucogaster*), a pantropical seabird species. *Chemosphere* 298, 134305. <https://doi.org/10.1016/j.chemosphere.2022.134305>.
- [43] Braune, B.M., Gaskin, D.E., 1987. Mercury levels in Bonaparte's gulls (*Larus Philadelphica*) during autumn molt in the Quoddy region, New Brunswick, Canada. *Arch Environ Contam Toxicol* 16, 539–549. <https://doi.org/10.1007/BF01055810>.
- [44] Schreiber, E.A., Feare, C.J., Harrington, B.A., Murray Jr., B.G., Robertson J., W. B., Robertson, Woolfenden, M.J., G.E., 2020. In: Billerman, S.M. (Ed.), *Sooty Tern (Onychoprion fuscatus)*, version 1.0. In *Birds of the World*. Cornell Lab of Ornithology, Ithaca, NY, USA. <https://doi.org/10.2173/bow.sooter1.01>.
- [45] Carravieri, A., Cherel, Y., Blévin, P., Brault-Favrou, M., Chastel, O., Bustamante, P., 2014. Mercury exposure in a large subantarctic avian community. *Environ Pollut* 190, 51–57. <https://doi.org/10.1016/j.envpol.2014.03.017>.
- [46] Kelly, J.F., 2000. Stable isotopes of carbon and nitrogen in the study of avian and mammalian trophic ecology. *Can J Zool* 78, 1–27. <https://doi.org/10.1139/z99-165>.
- [47] Burger, J., Gochfeld, M., 2001. Effects of chemicals and pollution on seabirds. In: *Biology of Marine Birds*. CRC Press, pp. 485–525. <https://doi.org/10.1201/9781420036305>.
- [48] Gochfeld, J.B., Michael, 2000. Effects of Lead on Birds (laridae): A review of laboratory and field studies. *J Toxicol Environ Health Part B* 3, 59–78. <https://doi.org/10.1080/109374000281096>.
- [49] Bond, A.L., Hobson, K.A., Branfireun, B.A., 2015. Rapidly increasing methyl mercury in endangered ivory gull (*Pagophila eburnea*) feathers over a 130 year record. *Proc Biol Sci* 282, 1–8.
- [50] Carravieri, A., Cherel, Y., Jaeger, A., Churlaud, C., Bustamante, P., 2016. Penguins as bioindicators of mercury contamination in the southern Indian Ocean: Geographical and temporal trends. *Environ Pollut Barking Essex* 1987 213, 195–205. <https://doi.org/10.1016/j.envpol.2016.02.010>.
- [51] Choy, E.S., Blight, L.K., Elliott, J.E., Hobson, K.A., Zanuttig, M., Elliott, K.H., 2022. Stable mercury trends support a long-term diet shift away from marine foraging in Salish Sea Glaucous-Winged Gulls over the last century. *Environ Sci Technol* 56, 12097–12105. <https://doi.org/10.1021/acs.est.1c03760>.
- [52] Fort, J., Grémillet, D., Traisnel, G., Amélineau, F., Bustamante, P., 2016. Does temporal variation of mercury levels in Arctic seabirds reflect changes in global environmental contamination, or a modification of Arctic marine food web

- functioning? *Environ Pollut* 211, 382–388. <https://doi.org/10.1016/j.envpol.2015.12.061>.
- [53] Ohkouchi, N., Chikaraishi, Y., Close, H.G., Fry, B., Larsen, T., Madigan, D.J., McCarthy, M.D., McMahon, K.W., Nagata, T., Naito, Y.I., Ogawa, N.O., Popp, B.N., Steffan, S., Takano, Y., Tayasu, I., Wyatt, A.S.J., Yamaguchi, Y.T., Yokoyama, Y., 2017. Advances in the application of amino acid nitrogen isotopic analysis in ecological and biogeochemical studies. *Org Geochem* 113, 150–174. <https://doi.org/10.1016/j.orggeochem.2017.07.009>.
- [54] Jardine, T.D., Kidd, K.A., Fisk, A.T., 2006. Applications, considerations, and sources of uncertainty when using stable isotope analysis in ecotoxicology. *Environ Sci Technol* 40, 7501–7511. <https://doi.org/10.1021/es061263h>.
- [55] McMahon, K.W., Hamady, L.L., Thorrold, S.R., 2013. Ocean ecogeochemistry: A review. *Oceanogr Mar Biol Annu Rev* 51, 327–374.
- [56] Popp, B.N., Graham, B.S., Olson, R.J., Hannides, C.C.S., Lott, M.J., López-Ibarra, G.A., Galván-Magaña, F., Fry, B., 2007. Insight into the trophic ecology of Yellowfin Tuna, *Thunnus albacares*, from compound-specific nitrogen isotope analysis of proteinaceous amino acids. In: *Terrestrial Ecology, Stable isotopes as indicators of ecological change*. Elsevier, pp. 173–190. [https://doi.org/10.1016/S1936-7961\(07\)01012-3](https://doi.org/10.1016/S1936-7961(07)01012-3).
- [57] McMahon, K.W., Newsome, S.D., 2019. Chapter 7 - Amino acid isotope analysis: A new frontier in studies of animal migration and foraging ecology, in: In: Hobson, K.A., Wassenaar, L.I. (Eds.), *Tracking Animal Migration with Stable Isotopes* (Second Edition). Academic Press, pp. 173–190. <https://doi.org/10.1016/B978-0-12-814723-8.00007-6>.
- [58] Chikaraishi, Y., Ogawa, N.O., Kashiyama, Y., Takano, Y., Suga, H., Tomitani, A., Miyashita, H., Kitazato, H., Ohkouchi, N., 2009. Determination of aquatic food-web structure based on compound-specific nitrogen isotopic composition of amino acids. *Limnol Oceanogr Methods* 7, 740–750. <https://doi.org/10.4319/lom.2009.7.740>.
- [59] Chikaraishi, Y., Steffan, S.A., Ogawa, N.O., Ishikawa, N.F., Sasaki, Y., Tsuchiya, M., Ohkouchi, N., 2014. High-resolution food webs based on nitrogen isotopic composition of amino acids. *Ecol Evol* 4, 2423–2449. <https://doi.org/10.1002/ece3.1103>.
- [60] Vihtakari M. (2024) ggOceanMaps: Plot data on oceanographic maps using 'ggplot2'. R package version 2.2.0. URL: (<https://CRAN.R-project.org/package=ggOceanMaps>)>
- [61] Carravieri, A., Bustamante, P., Churlaud, C., Fromant, A., Cherel, Y., 2014. Moulting patterns drive within-individual variations of stable isotopes and mercury in seabird body feathers: Implications for monitoring of the marine environment. *Mar Biol* 161, 963–968. <https://doi.org/10.1007/s00227-014-2394-x>.
- [62] Jaeger, A., Blanchard, P., Richard, P., Cherel, Y., 2009. Using carbon and nitrogen isotope values of body feathers to infer inter- and intra-individual variations of seabird feeding ecology during moult. *Mar Biol* 156, 1233–1240. <https://doi.org/10.1007/s00227-009-1165-6>.
- [63] Cusset, F., Reynolds, S.J., Carravieri, A., Amouroux, D., Asensio, O., Dickey, R.C., Fort, J., Hughes, B.J., Paiva, V.H., Ramos, J.A., Shearer, L., Tessier, E., Wearn, C. P., Cherel, Y., Bustamante, P., 2023. A century of mercury: Ecosystem-wide changes drive increasing contamination of a tropical seabird species in the South Atlantic Ocean. *Environ Pollut*, 121187. <https://doi.org/10.1016/j.envpol.2023.121187>.
- [64] Renedo, M., Bustamante, P., Tessier, E., Pedrero, Z., Cherel, Y., Amouroux, D., 2017. Assessment of mercury speciation in feathers using species-specific isotope dilution analysis. *Talanta* 174, 100–110. <https://doi.org/10.1016/j.talanta.2017.05.081>.
- [65] Styring, A.K., Kuhl, A., Knowles, T.D.J., Fraser, R.A., Bogaard, A., Evershed, R.P., 2012. Practical considerations in the determination of compound-specific amino acid $\delta^{15}\text{N}$ values in animal and plant tissues by gas chromatography-combustion-isotope ratio mass spectrometry, following derivatisation to their N-acetylpropyl esters. *Rapid Commun Mass Spectrom* 26, 2328–2334. <https://doi.org/10.1002/rcm.6322>.
- [66] Corr, L.T., Berstan, R., Evershed, R.P., 2007. Development of N-acetyl methyl ester derivatives for the determination of $\delta^{13}\text{C}$ values of amino acids using gas chromatography-combustion-isotope ratio Mass Spectrometry. *Anal Chem* 79, 9082–9090. <https://doi.org/10.1021/ac071223b>.
- [67] Sabadel, A.J.M., Woodward, E.M.S., Van Hale, R., Frew, R.D., 2016. Compound-specific isotope analysis of amino acids: A tool to unravel complex symbiotic trophic relationships. *Food Webs* 6, 9–18. <https://doi.org/10.1016/j.fooweb.2015.12.003>.
- [68] Yarnes, C.T., Herszage, J., 2017. The relative influence of derivatization and normalization procedures on the compound-specific stable isotope analysis of nitrogen in amino acids. *Rapid Commun Mass Spectrom* 31, 693–704. <https://doi.org/10.1002/rcm.7832>.
- [69] Ashmole, N.P., 1963. The Biology of the Wakeful or Sooty Tern *Sterna Fuscata* on Ascension Island. *Ibis* 103b, 297–351. <https://doi.org/10.1111/j.1474-919X.1963.tb06757.x>.
- [70] Reynolds, S.J., Martin, G.R., Dawson, A., Wearn, C.P., Hughes, B.J., 2014. The sub-annual breeding cycle of a tropical seabird. *PLoS ONE* 9. <https://doi.org/10.1371/journal.pone.0093582>.
- [71] Neumann, J., Larose, C.S., Brodin, G., Feare, C.J., 2018. Foraging ranges of incubating sooty terns *Onychoprion fuscatus* on Bird Island, Seychelles, during a transition from food plenty to scarcity, as revealed by GPS loggers. *Mar Ornithol* 46, 11–18.
- [72] Oppel, S., Bolton, M., Carneiro, A.P.B., Dias, M.P., Green, J.A., Masello, J.F., Phillips, R.A., Owen, E., Quillfeldt, P., Beard, A., Bertrand, S., Blackburn, J., Boersma, P.D., Borges, A., Broderick, A.C., Catry, P., Cleasby, I., Clingham, E., Creuwels, J., Crofts, S., Cuthbert, R.J., Dallmeijer, H., Davies, D., Davies, R., Dilley, B.J., Dinis, H.A., Dossa, J., Dunn, M.J., Efe, M.A., Fayet, A.L., Figueiredo, L., Frederico, A.P., Gjerdrum, C., Godley, B.J., Granadeiro, J.P., Guilford, T., Hamer, K.C., Hazin, C., Hedd, A., Henry, L., Hernández-Montero, M., Hinke, J., Kokubun, N., Leat, E., Tranquilla, L.M., Metzger, B., Militao, T., Montrond, G., Mullié, W., Padgett, O., Pearmain, E.J., Pollet, I.L., Pütz, K., Quintana, F., Ratcliffe, N., Ronconi, R.A., Ryan, P.G., Saldanha, S., Shoji, A., Sim, J., Small, C., Soanes, L., Takahashi, A., Trathan, P., Trivelpiece, W., Veen, J., Wakefield, E., Weber, N., Weber, S., Zango, L., Daunt, F., Ito, M., Harris, M.P., Newell, M.A., Wanless, S., González-Solis, J., Croxall, J., 2018. Spatial scales of marine conservation management for breeding seabirds. *Mar Policy* 98, 37–46. <https://doi.org/10.1016/j.marpol.2018.08.024>.
- [73] Soanes, L.M., Bright, J.A., Brodin, G., Mukhida, F., Green, J.A., 2015. Tracking a small seabird: First records of foraging behaviour in the Sooty Tern *Onychoprion fuscatus*. *Mar Ornithol* 43, 235–239.
- [74] Soanes, L.M., Bright, J.A., Carter, D., Dias, M.P., Fleming, T., Gumbs, K., Hughes, G., Mukhida, F., Green, J.A., 2016. Important foraging areas of seabirds from Anguilla, Caribbean: Implications for marine spatial planning. *Mar Policy* 70, 85–92. <https://doi.org/10.1016/j.marpol.2016.04.019>.
- [75] Reynolds, S.J., Wearn, C.P., Hughes, B.J., Dickey, R.C., Garrett, L.J.H., Walls, S., Hughes, F.T., Weber, N., Weber, S.B., Leat, E.H.K., Andrews, K., Ramos, J.A., Paiva, V.H., 2021. Year-round movements of Sooty Terns (*Onychoprion fuscatus*) nesting within one of the Atlantic's largest Marine Protected Areas. *Front Mar Sci* 8.
- [76] Jaeger, A., Feare, C.J., Summers, R.W., Lebarbenchon, C., Larose, C.S., Le Corre, M., 2017. Geolocation reveals year-round at-sea distribution and activity of a superabundant tropical seabird, the Sooty Tern *Onychoprion fuscatus*. *Front Mar Sci* 4. <https://doi.org/10.3389/fmars.2017.00394>.
- [77] Hobson, K.A., Clark, R.G., 1992. Assessing avian diets using stable isotopes I: Turnover of ^{13}C in tissues. *Condor* 94, 181–188. <https://doi.org/10.2307/1368807>.
- [78] Bond, A.L., 2010. Relationships between stable isotopes and metal contaminants in feathers are spurious and biologically uninformative. *Environ Pollut* 158, 1182–1184. <https://doi.org/10.1016/j.envpol.2010.01.004>.
- [79] Blévin, P., Carravieri, A., Jaeger, A., Chastel, O., Bustamante, P., Cherel, Y., 2013. Wide range of mercury contamination in chicks of Southern Ocean seabirds. *PLOS ONE* 8, e54508. <https://doi.org/10.1371/journal.pone.0054508>.
- [80] Stewart, F., Phillips, R., Catry, P., Furness, R., 1997. Influence of species, age and diet on mercury concentrations in Shetland seabirds. *Mar Ecol Prog Ser* 151, 237–244. <https://doi.org/10.3354/meps151237>.
- [81] Lorrain, A., Graham, B., Ménard, F., Popp, B., Bouillon, S., Breugel, P., van, Cherel, Y., 2009. Nitrogen and carbon isotope values of individual amino acids: A tool to study foraging ecology of penguins in the Southern Ocean. *Mar Ecol Prog Ser* 391, 293–306. <https://doi.org/10.3354/meps08215>.
- [82] McClelland, J.W., Montoya, J.P., 2002. Trophic relationships and the nitrogen isotopic composition of amino acids in plankton. *Ecology* 83, 2173–2180. [https://doi.org/10.1890/0012-9658\(2002\)083\[2173:TRATN\]2.0.CO;2](https://doi.org/10.1890/0012-9658(2002)083[2173:TRATN]2.0.CO;2).
- [83] McMahon, K.W., McCarthy, M.D., 2016. Embracing variability in amino acid $\delta^{15}\text{N}$ fractionation: Mechanisms, implications, and applications for trophic ecology. *Ecosphere* 7, e01511. <https://doi.org/10.1002/ece3.1511>.
- [84] McMahon, K.W., Polito, M.J., Abel, S., McCarthy, M.D., Thorrold, S.R., 2015. Carbon and nitrogen isotope fractionation of amino acids in an avian marine predator, the gentoo penguin (*Pygoscelis papua*). *Ecol Evol* 5, 1278–1290. <https://doi.org/10.1002/ece3.1437>.
- [85] Quillfeldt, P., Masello, J.F., 2020. Compound-specific stable isotope analyses in Falkland Islands seabirds reveal seasonal changes in trophic positions. *BMC Ecol* 20, 21. <https://doi.org/10.1186/s12898-020-00288-5>.
- [86] R Core Team, 2022. R: A language and environment for statistical computing. R Foundation for Statistical Computing, Vienna, Austria. (<https://www.R-project.org/>) (URL).
- [87] Wickham, H., 2016. *ggplot2: Elegant graphics for data analysis*. Springer-Verlag, New York.
- [88] Zeileis, A., Hothorn, T., 2002. "Diagnostic Checking in Regression Relationships". *R N* 2 (3), 7–10 (URL: <https://CRAN.R-project.org/doc/Rnews/>).
- [89] Pinheiro, J., Bates, D., Core Team, R., Core Team, R., 2022. nlme: Linear and nonlinear mixed effects models. R Package Version 3, 1–160 (<https://svn.r-project.org/R-packages/trunk/nlme/>).
- [90] Barton, K., 2022. MuMIn: Multi-model inference. R Package Version, 1.47.5. URL: <https://CRAN.R-project.org/package=MuMIn>.
- [91] Burnham, K.P., Anderson, D.R., 2002. *Model selection and multimodal inference: A practical information – theoretic approach* (second ed). Springer, US.
- [92] Johnson, J.B., Omland, K.S., 2004. Model selection in ecology and evolution (<https://doi.org/>). *Trends Ecol Evol* 19, 101–108. <https://doi.org/10.1016/j.tree.2003.10.013>.
- [93] Length, R., 2024. emmeans Estim Marg means aka leastSq means R Package Version 1 10 0 URL. (<https://CRAN.R-project.org/package=emmeans>).
- [94] Bond, A.L., Diamond, A.W., 2009. Mercury concentrations in seabird tissues from Machias Seal Island, New Brunswick, Canada. *Sci Total Environ* 407, 4340–4347. <https://doi.org/10.1016/j.scitotenv.2009.04.018>.
- [95] Fox, J., Weisberg, S., 2018. Visualizing fit and lack of fit in complex regression models with predictor effect plots and partial residuals. *J Stat Softw* 87 (9), 1–27. <https://doi.org/10.18637/jss.v087.i09>.
- [96] Fox, J., Weisberg, S., 2019. R Companion Appl Regres 3rd Ed Thousands Oaks Ca URL. (<https://socialsciences.mcmaster.ca/jfox/Books/Companion/index.html>).
- [97] Burger, J., Shukla, T., Dixon, C., Shukla, S., McMahon, M.J., Ramos, R., Gochfeld, M., 2001. Metals in feathers of Sooty Tern, White Tern, Gray-Backed

- Tern, and Brown Noddy from Islands in the North Pacific. *Environ Monit Assess* 71, 71–89. <https://doi.org/10.1023/A:1011695829296>.
- [98] Burger, J., Gochfeld, M., 2000. Metal levels in feathers of 12 species of seabirds from Midway Atoll in the northern Pacific Ocean. *Sci Total Environ* 257, 37–52. [https://doi.org/10.1016/S0048-9697\(00\)00496-4](https://doi.org/10.1016/S0048-9697(00)00496-4).
- [99] Burger, J., Schreiber, E.A.E., Gochfeld, M., 1992. Lead, cadmium, selenium and mercury in seabird feathers from the tropical mid-Pacific. *Environ Toxicol Chem* 11, 815–822. <https://doi.org/10.1002/etc.5620110610>.
- [100] Burger, J., Gochfeld, M., 1991. Lead, mercury, and cadmium in feathers of tropical terns in Puerto Rico and Australia. *Arch Environ Contam Toxicol* 21, 311–315. <https://doi.org/10.1007/BF01055351>.
- [101] Kojadinovic, J., Bustamante, P., Churlaud, C., Cosson, R.P., Le Corre, M., 2007. Mercury in seabird feathers: Insight on dietary habits and evidence for exposure levels in the western Indian Ocean. *Sci Total Environ* 384, 194–204. <https://doi.org/10.1016/j.scitotenv.2007.05.018>.
- [102] Ramos, J.A., Tavares, P.C., 2010. Mercury levels in the feathers of breeding seabirds in the Seychelles, western Indian Ocean, from 1996 to 2005. *Emu Austral Ornithol* 110, 87–91. <https://doi.org/10.1071/MU09055>.
- [103] Jaquemet, S., Potier, M., Chérel, Y., Kojadinovic, J., Bustamante, P., Richard, P., Catry, T., Ramos, J.A., Le Corre, M., 2008. Comparative foraging ecology and ecological niche of a superabundant tropical seabird: The sooty tern *Sterna fuscata* in the southwest Indian Ocean. *Mar Biol* 155, 505–520. <https://doi.org/10.1007/s00227-008-1049-1>.
- [104] Burger, J., Gochfeld, M., 1995. Biomonitoring of heavy metals in the Pacific basin using avian feathers. *Environ Toxicol Chem* 14, 1233–1239. <https://doi.org/10.1002/etc.5620140716>.
- [105] Catry, T., Ramos, J.A., Le Corre, M., Kojadinovic, J., Bustamante, P., 2008. The role of stable isotopes and mercury concentrations to describe seabird foraging ecology in tropical environments. *Mar Biol* 155, 637–647. <https://doi.org/10.1007/s00227-008-1060-6>.
- [106] Monticelli, D., Ramos, J.A., Tavares, P.C., Bataille, B., Lepoint, G., Devillers, P., 2008. Diet and foraging ecology of Roseate Terns and Lesser Noddies breeding sympatrically on Aride Island, Seychelles. *Waterbirds* 31, 231–240. [https://doi.org/10.1675/1524-4695\(2008\)31\[231:DAFEOR\]2.0.CO;2](https://doi.org/10.1675/1524-4695(2008)31[231:DAFEOR]2.0.CO;2).
- [107] Reynolds, S.J., Hughes, B.J., Wearn, C.P., Dickey, R.C., Brown, J., Weber, N.L., Weber, S.B., Paiva, V.H., Ramos, J.A., 2019. Long-term dietary shift and population decline of a pelagic seabird—A health check on the tropical Atlantic? *Glob Change Biol* 25, 1383–1394. <https://doi.org/10.1111/gcb.14560>.
- [108] Monteiro, L.R., Furness, R.W., 1997. Accelerated increase in mercury contamination in north Atlantic mesopelagic food chains as indicated by time series of seabird feathers. *Environ Toxicol Chem* 16, 2489–2493. <https://doi.org/10.1002/etc.5620161208>.
- [109] Ochoa-Acuña, H., Sepúlveda, M.S., Gross, T.S., 2002. Mercury in feathers from Chilean birds: Influence of location, feeding strategy, and taxonomic affiliation. *Mar Pollut Bull* 44, 340–345. [https://doi.org/10.1016/S0025-326X\(01\)00280-6](https://doi.org/10.1016/S0025-326X(01)00280-6).
- [110] Chouvelon, T., Spitz, J., Caurant, F., Méndez-Fernandez, P., Autier, J., Lassus-Débat, A., Chappuis, A., Bustamante, P., 2012. Enhanced bioaccumulation of mercury in deep-sea fauna from the Bay of Biscay (north-east Atlantic) in relation to trophic positions identified by analysis of carbon and nitrogen stable isotopes. *Deep Sea Res Part Oceanogr Res Pap* 65, 113–124. <https://doi.org/10.1016/j.dsr.2012.02.010>.
- [111] Fisher, J.A., Schneider, L., Fostier, A.-H., Guerrero, S., Guimarães, J.R.D., Labuschagne, C., Leaner, J.J., Martin, L.G., Mason, R.P., Somerset, V., Walters, C., 2023. A synthesis of mercury research in the Southern Hemisphere, part 2: Anthropogenic perturbations. *Ambio*. <https://doi.org/10.1007/s13280-023-01840-5>.
- [112] Hylander, L.D., Meili, M., 2003. 500 years of mercury production: Global annual inventory by region until 2000 and associated emissions. *Sci Total Environ Pathw Process Mercury Environ Sel Pap Presente sixth Int Conf Mercury Glob Pollut Minamata Jpn Oct 1519 2001 (304)*, 13–27. [https://doi.org/10.1016/S0048-9697\(02\)00553-3](https://doi.org/10.1016/S0048-9697(02)00553-3).
- [113] Li, C., Sonke, J.E., Le Roux, G., Piotrowska, N., Van der Putten, N., Roberts, S.J., Daley, T., Rice, E., Gehrels, R., Enrico, M., Mauquoy, D., Roland, T.P., De Vleeschouwer, F., 2020. Unequal anthropogenic enrichment of mercury in Earth's Northern and Southern Hemispheres. *ACS Earth Space Chem*. <https://doi.org/10.1021/acsearthspacechem.0c00220>.
- [114] Médiéu, A., Point, D., Itai, T., Angot, H., Buchanan, P.J., Allain, V., Fuller, L., Griffiths, S., Gillikin, D.P., Sonke, J.E., Heimbürger-Boavida, L.-E., Desgranges, M.-M., Menkes, C.E., Madigan, D.J., Brosset, P., Gauthier, O., Tagliabue, A., Bopp, L., Verheyden, A., Lorrain, A., 2022. Evidence that Pacific tuna mercury levels are driven by marine methylmercury production and anthropogenic inputs. *Proc Natl Acad Sci* 119, e2113032119. <https://doi.org/10.1073/pnas.2113032119>.
- [115] Médiéu, A., Lorrain, A., Point, D., 2023. Are tunas relevant bioindicators of mercury concentrations in the global ocean? *Ecotoxicology*. <https://doi.org/10.1007/s10646-023-02679-y>.
- [116] Liu, M., Zhang, Q., Maavara, T., Liu, S., Wang, X., Raymond, P.A., 2021. Rivers as the largest source of mercury to coastal oceans worldwide. *Nat Geosci* 14, 672–677. <https://doi.org/10.1038/s41561-021-00793-2>.
- [117] Somoza, L., Medialdea, T., González, F.J., Calado, A., Afonso, A., Albuquerque, M., Asensio-Ramos, M., Bettencourt, R., Blasco, I., Candón, J.A., Carreiro-Silva, M., Cid, C., De Ignacio, C., López-Pamo, E., Machancoses, S., Ramos, B., Ribeiro, L.P., Rincón-Tomás, B., Santofimia, E., Souto, M., Tojeira, I., Viegas, C., Madureira, P., 2020. Multidisciplinary scientific cruise to the northern mid-atlantic ridge and azores archipelago. *Front Mar Sci* 7. <https://doi.org/10.3389/fmars.2020.568035>.
- [118] Vieira, H.C., Bordalo, M.D., Osten, J.R., Soares, A.M.V.M., Abreu, S.N., Morgado, F., 2023. Can a 16th Century Shipwreck Be Considered a Mercury Source in the 21st Century? - A Case Study in the Azores Archipelago (Portugal). *J Mar Sci Eng* 11, 276. <https://doi.org/10.3390/jmse11020276>.
- [119] Feng, C., Pedrero, Z., Lima, L., Olivares, S., de la Rosa, D., Beraíl, S., Tessier, E., Pannier, F., Amouroux, D., 2019. Assessment of Hg contamination by a Chlor-Alkali Plant in riverine and coastal sites combining Hg speciation and isotopic signature (Sagua la Grande River, Cuba). *J Hazard Mater* 371, 558–565. <https://doi.org/10.1016/j.jhazmat.2019.02.092>.
- [120] Brasso, R.L., Chiaradia, A., Polito, M.J., Raya Rey, A., Emslie, S.D., 2015. A comprehensive assessment of mercury exposure in penguin populations throughout the Southern Hemisphere: using trophic calculations to identify sources of population-level variation. *Mar Pollut Bull* 97, 408–418. <https://doi.org/10.1016/j.marpolbul.2015.05.059>.
- [121] Gatt, M.C., Reis, B., Granadeiro, J.P., Pereira, E., Catry, P., 2020. Generalist seabirds as biomonitoring of ocean mercury: The importance of accurate trophic position assignment. *Sci Total Environ* 740, 140159. <https://doi.org/10.1016/j.scitotenv.2020.140159>.
- [122] Post, D.M., 2002. Using stable isotopes to estimate trophic position: Models, methods, and assumptions. *Ecology* 83, 703–718. [https://doi.org/10.1890/0012-9658\(2002\)083\[0703:USITET\]2.0.CO;2](https://doi.org/10.1890/0012-9658(2002)083[0703:USITET]2.0.CO;2).
- [123] Quillfeldt, P., Masello, J.F., McGill, R.A., Adams, M., Furness, R.W., 2010. Moving polewards in winter: A recent change in the migratory strategy of a pelagic seabird? *Front Zool* 7, 15. <https://doi.org/10.1186/1742-9994-7-15>.
- [124] Carravieri, A., Bustamante, P., Tartu, S., Meillère, A., Labadie, P., Budzinski, H., Peluhet, L., Barbraud, C., Weimerskirch, H., Chastel, O., Chérel, Y., 2014. Wandering Albatrosses document latitudinal variations in the transfer of persistent organic pollutants and mercury to Southern Ocean predators. *Environ Sci Technol* 48, 14746–14755. <https://doi.org/10.1021/es504601m>.
- [125] Chérel, Y., Hobson, K.A., 2007. Geographical variation in carbon stable isotope signatures of marine predators: A tool to investigate their foraging areas in the Southern Ocean. *Mar Ecol Prog Ser* 329, 281–287. <https://doi.org/10.3354/meps329281>.
- [126] Stenhouse, I.J., Egevang, C., Phillips, R.A., 2012. Trans-equatorial migration, staging sites and wintering area of Sabine's Gulls *Larus sabini* in the Atlantic Ocean. *Ibis* 154, 42–51. <https://doi.org/10.1111/j.1474-919X.2011.01180.x>.
- [127] Carey, M.J., Phillips, R.A., Silk, J.R.D., Shaffer, S.A., 2014. Trans-equatorial migration of Short-tailed Shearwaters revealed by geolocators. *Emu Austral Ornithol* 114, 352–359. <https://doi.org/10.1071/MU13115>.
- [128] González-Solís, J., Croxall, J.P., Oro, D., Ruiz, X., 2007. Trans-equatorial migration and mixing in the wintering areas of a pelagic seabird. *Front Ecol Environ* 5, 297–301. [https://doi.org/10.1890/1540-9295\(2007\)5\[297:TMAMIT\]2.0.CO;2](https://doi.org/10.1890/1540-9295(2007)5[297:TMAMIT]2.0.CO;2).
- [129] Baak, J.E., Provencher, J.F., Mallory, M.L., Elliott, K.H., 2024. Spatial ecotoxicology: What we know about the relationship between avian movements and contaminant levels. *Environ Rev* 32, 315–333. <https://doi.org/10.1139/er-2023-0101>.
- [130] Olivier, L., Reverdin, G., Boutin, J., Laxenaire, R., Iudicone, D., Pesant, S., Calil, P. H.R., Horstmann, J., Couet, D., Ertza, J.M., Huber, P., Sarmiento, H., Freire, A., Koch-Larrouy, A., Vergely, J.-L., Rousselot, P., Speich, S., 2024. Late summer northward Amazon plume pathway under the action of the North Brazil Current rings. *Remote Sens Environ* 307, 114165. <https://doi.org/10.1016/j.rse.2024.114165>.
- [131] Thompson, D.R., Furness, R.W., Walsh, P.M., 1992. Historical Changes in mercury concentrations in the marine ecosystem of the North and North-East Atlantic Ocean as indicated by seabird feathers. *J Appl Ecol* 29, 79–84. <https://doi.org/10.2307/2404350>.
- [132] Vo, A.-T.E., Bank, M.S., Shine, J.P., Edwards, S.V., 2011. Temporal increase in organic mercury in an endangered pelagic seabird assessed by century-old museum specimens. *Proc Natl Acad Sci* 108, 7466–7471. <https://doi.org/10.1073/pnas.1013865108>.
- [133] Hensley, V.I., Hensley, D.A., 1995. Fishes Eaten by Sooty Terns and Brown Noddies in the Dry Tortugas, Florida. *Bull Mar Sci* 56, 813–821.
- [134] Décima, M., Landry, M.R., Popp, B.N., 2013. Environmental perturbation effects on baseline $\delta^{15}\text{N}$ values and zooplankton trophic flexibility in the southern California Current Ecosystem. *Limnol Oceanogr* 58, 624–634. <https://doi.org/10.4319/lo.2013.58.2.0624>.
- [135] Hannides, C.C.S., Popp, B.N., Landry, M.R., Graham, B.S., 2009. Quantification of zooplankton trophic position in the North Pacific Subtropical Gyre using stable nitrogen isotopes. *Limnol Oceanogr* 54, 50–61. <https://doi.org/10.4319/lo.2009.54.1.0050>.
- [136] Sigman, D., 2009. Nitrogen isotopes in the ocean. *Encycl Ocean Sci*. <https://doi.org/10.1016/B978-012374473-9.00632-9>.
- [137] García-Seoane, R., Viana, I.G., Bode, A., 2023. Seasonal upwelling influence on trophic indices of mesozooplankton in a coastal food web estimated from $\delta^{15}\text{N}$ in amino acids. *Prog Oceanogr* 219, 103149. <https://doi.org/10.1016/j.pocan.2023.103149>.
- [138] Bowman, K.L., Hammerschmidt, C.R., Lamborg, C.H., Swarr, G.J., Agather, A.M., 2016. Distribution of mercury species across a zonal section of the eastern tropical South Pacific Ocean (U.S. GEOTRACES GP16). *Mar Chem* 186, 156–166. <https://doi.org/10.1016/j.marchem.2016.09.005>.
- [139] Cossa, D., Cotté-Krief, M.-H., Mason, R.P., Bretaudeau-Sanjuan, J., 2004. Total mercury in the water column near the shelf edge of the European continental margin. In: *Mar. Chem*, 90. Special Issue in honor of Dr. William F. Fitzgerald, pp. 21–29. <https://doi.org/10.1016/j.marchem.2004.02.019>.

- [140] Mason, R.P., Fitzgerald, W.F., 1993. The distribution and biogeochemical cycling of mercury in the equatorial Pacific Ocean. *Deep Sea Res Part Oceanogr Res Pap* 40, 1897–1924. [https://doi.org/10.1016/0967-0637\(93\)90037-4](https://doi.org/10.1016/0967-0637(93)90037-4).
- [141] Pires, A., Ramos, S., Aguilera, O., Garnier, J., Kawakami, S., Almeida, E., Martinelli, J.E., Silva-Filho, E., Albuquerque, A.L., Kütter, V., 2025. Mercury and selenium in biological pump under upwelling-downwelling influence in Cabo Frio shelf, South Atlantic Ocean, Brazil. *Sci Total Environ* 959, 178295. <https://doi.org/10.1016/j.scitotenv.2024.178295>.
- [142] Galvao, P., Sus, B., Lailson-Brito, J., Azevedo, A., Malm, O., Bisi, T., 2021. An upwelling area as a hot spot for mercury biomonitoring in a climate change scenario: A case study with large demersal fishes from Southeast Atlantic (SE-Brazil). *Chemosphere* 269, 128718. <https://doi.org/10.1016/j.chemosphere.2020.128718>.
- [143] Sunderland, E.M., Mason, R.P., 2007. Human impacts on open ocean mercury concentrations. *Glob Biogeochem Cycles* 21. <https://doi.org/10.1029/2006GB002876>.
- [144] Foster, K.L., Braune, B.M., Gaston, A.J., Mallory, M.L., 2019. Climate influence on mercury in Arctic seabirds. *Sci Total Environ* 693, 133569. <https://doi.org/10.1016/j.scitotenv.2019.07.375>.
- [145] Sonke, J.E., Angot, H., Zhang, Y., Poulain, A., Björn, E., Schartup, A., 2023. Global change effects on biogeochemical mercury cycling. *Ambio*. <https://doi.org/10.1007/s13280-023-01855-y>.